

AD-A142 200

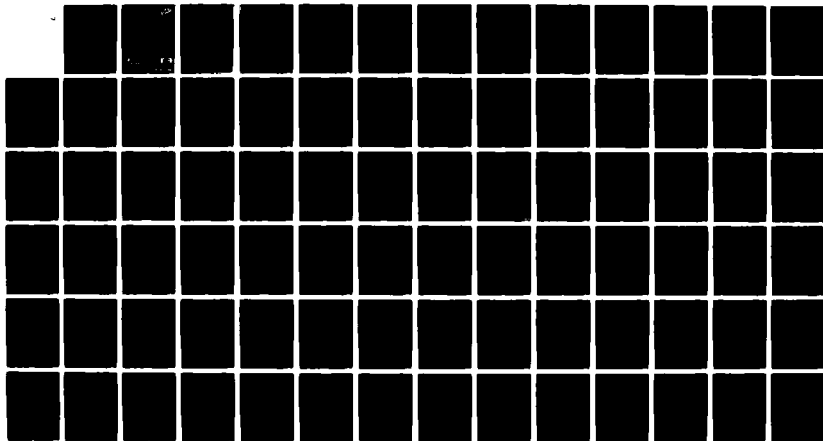
A THREE-DIMENSIONAL DYNAMICAL-CHEMICAL MODEL OF THE
MESOSPHERE AND LOWER... (U) GEORGIA INST OF TECH ATLANTA
SCHOOL OF GEOPHYSICAL SCIENCES F N ALYEA 20 JAN 84
AFGL-TR-84-0070 F19628-81-K-0045

1/1

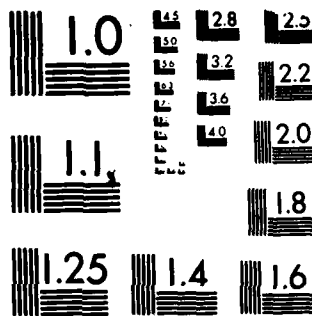
NL

UNCLASSIFIED

F/G 4/1



END
DATE
FILMED
7-84
DTIC



MICROCOPY RESOLUTION TEST CHART
NATIONAL BUREAU OF STANDARDS-1963-A

AD-A142 200

②

AFGL-TR-84-0070

A THREE-DIMENSIONAL DYNAMICAL-CHEMICAL
MODEL OF THE MESOSPHERE AND LOWER
THERMOSPHERE FOR UPPER ATMOSPHERIC RESEARCH

Fred N. Alyea

Georgia Institute of Technology
School of Geophysical Sciences
Atlanta, Georgia 30332

20 January 1984

Final Report
18 May 1981 - 30 September 1983

Approved for public release; distribution unlimited


DTIC FILE COPY

AIR FORCE GEOPHYSICS LABORATORY
AIR FORCE SYSTEMS COMMAND
WRIGHT PATTEN AIR FORCE
WRIGHT PATTEN AIR FORCE 01731

DTIC
ELECTE
JUN 18 1984
S D

This report has been reviewed by the ESD Public Affairs Office (PA) and is releasable to the National Technical Information Service (NTIS).

This technical report has been reviewed and is approved for publication.



(Signature)

Thomas J. Kaneshea
Lab. Contract Manager


(Signature)

K.S.W. Champion
Chief, Global Density Branch

FOR THE COMMANDER


(Signature)

Robert A. McClatchey
Director, Atmospheric Sciences Division

Qualified requestors may obtain additional copies from the Defense Technical Information Center. All others should apply to the National Technical Information Service.

If your address has changed, or if you wish to be removed from the mailing list, or if the addressee is no longer employed by your organization, please notify AFGL/DAA, Hanscom AFB, MA 01731. This will assist us in maintaining a current mailing list.

Do not return copies of this report unless contractual obligations or notices on a specific document require that it be returned.

REPORT DOCUMENTATION PAGE

1a. REPORT SECURITY CLASSIFICATION Unclassified		1b. RESTRICTIVE MARKINGS			
2a. SECURITY CLASSIFICATION AUTHORITY		3. DISTRIBUTION/AVAILABILITY OF REPORT Approved for public release; distribution unlimited			
2b. DECLASSIFICATION/DOWNGRADING SCHEDULE					
4. PERFORMING ORGANIZATION REPORT NUMBER(S)		5. MONITORING ORGANIZATION REPORT NUMBER(S) AFGL-TR-84-0070			
6a. NAME OF PERFORMING ORGANIZATION Georgia Institute of Technology School of Geophysical Sciences	6b. OFFICE SYMBOL (If applicable)	7a. NAME OF MONITORING ORGANIZATION Air Force Geophysics Laboratory			
6c. ADDRESS (City, State and ZIP Code) Atlanta, Georgia 30332		7b. ADDRESS (City, State and ZIP Code) Hanscom AFB, Massachusetts 01731 Monitor/Thomas J. Keneshea/LKB			
8a. NAME OF FUNDING/SPONSORING ORGANIZATION	8b. OFFICE SYMBOL (If applicable)	9. PROCUREMENT INSTRUMENT IDENTIFICATION NUMBER F19628-81-K-0045			
8c. ADDRESS (City, State and ZIP Code)		10. SOURCE OF FUNDING NOS.			
		PROGRAM ELEMENT NO. 62101F	PROJECT NO. 6690	TASK NO. 07	WORK UNIT NO. AH
11. TITLE (Include Security Classification) (over)					
12. PERSONAL AUTHOR(S) Alvea, Fred N.					
13a. TYPE OF REPORT Final Report	13b. TIME COVERED FROM 5-18-81 TO 9-30-83	14. DATE OF REPORT (Yr., Mo., Day) 20 January 1984	15. PAGE COUNT 86		
16. SUPPLEMENTARY NOTATION					
17. COSATI CODES			18. SUBJECT TERMS (Continue on reverse if necessary and identify by block number)		
FIELD	GROUP	SUB. GR.	atmospheric modeling, mesosphere, thermosphere, atmospheric dynamics		
19. ABSTRACT (Continue on reverse if necessary and identify by block number)					
<p>The recent appearance of new observational data from specialized satellites and rocket probes has led to increased interest in upper atmospheric processes. The work to be reported herein is of the current status of a limited three-dimensional model of the dynamical and important chemical processes which are known to take place in the mesosphere and lower thermosphere to an altitude of about 400 km above the earth's surface.</p> <p>The modeling approach taken was to make use of the dynamical schemes and simplified chemical treatments embodied in our three-dimensional Stratospheric Circulation Model (SCM) developed for the study of stratospheric ozone (see Cunnold et al., 1975). The basic strategy in the modeling effort was to use the modified SCM codes to specify the large scale dynamical properties of the upper atmospheric region and for the integration of the time dependent, three-dimensional mass continuity equations for the chemically active species. Development of the chemical and sub-scale transport properties of the model were to be (over)</p>					
20. DISTRIBUTION/AVAILABILITY OF ABSTRACT UNCLASSIFIED/UNLIMITED <input checked="" type="checkbox"/> SAME AS RPT. <input type="checkbox"/> DTIC USERS <input type="checkbox"/>			21. ABSTRACT SECURITY CLASSIFICATION Unclassified		
22a. NAME OF RESPONSIBLE INDIVIDUAL Thomas J. Keneshea/LKB		22b. TELEPHONE NUMBER (Include Area Code)	22c. OFFICE SYMBOL LKB		

Unclassified

SECURITY CLASSIFICATION OF THIS PAGE

Block 11 (Contd)

A THREE-DIMENSIONAL DYNAMICAL-CHEMICAL MODEL OF THE MESOSPHERE AND
LOWER THERMOSPHERE FOR UPPER ATMOSPHERIC RESEARCH

Block 19 (Contd)

undertaken by the AFGL group under the direction of Dr. S. P. Zimmerman. Thus, the complete modeling program was devised to be a cooperative venture between Georgia Tech and AFGL.

Unclassified

SECURITY CLASSIFICATION OF THIS PAGE

Table of Contents

Introduction 0-1

Accomplishments 0-3

 A. Model heating 0-3

 B. Model lower boundary conditions 0-8

 C. Dynamical tests 0-10

1. Basic dynamical equations and coordinate system 1-1

2. Choice of vertical levels 2-1

3. Non-dimensional finite-difference equations 3-1

4. Spectral form of the equations 4-1

5. Determination of W in the dynamic equations 5-1

6. The model codes 6-1

Appendix A. Spectral form of Jacobian terms and evaluation of
the associated nonlinear interaction coefficients A-1

Appendix B. Spectral representation of divergence terms of the
form $\nabla \cdot \mu \nabla A$ B-1

Appendix C. Solution of a tridiagonal set of equations C-1

Appendix D. Computation of the weight functions for Gaussian
quadrature D-1

Accession For	
NTIS GRA&I	<input checked="" type="checkbox"/>
DTIC TAB	<input type="checkbox"/>
Unannounced	<input type="checkbox"/>
Justification	
By _____	
Distribution/	
Availability Codes	
Dist	Avail and/or Special
A/1	



0. Introduction and Accomplishments

Introduction

→ The recent appearance of new observational data from specialized satellites and rocket probes has led to increased interest in upper atmospheric processes. The work to be reported herein is of the current status of a limited three-dimensional model of the dynamical and important chemical processes which are known to take place in the mesosphere and lower thermosphere to an altitude of about 400 km above the earth's surface. Unfortunately, funds for the program were cut off prior to its completion and thus the model codes have not been finalized. It is hoped that this program can be picked up again in the near future.

→ The modeling approach taken was to make use of the dynamical schemes and simplified chemical treatments embodied in our three-dimensional Stratospheric Circulation Model (SCM) developed for the study of stratospheric ozone, (see Cunnold, et al., 1975). This model has been running on the now defunct ILLIAC-4 vector computer at NASA's Ames Research Center in California. In addition to large changes required in the existing dynamics and chemistry to reform the model for thermospheric and mesospheric levels, it was also necessary to revise the code structure to accommodate the shift from the ILLIAC machine to the AFGL CDC-660 computer. Much of this work was accomplished on the NASA machines prior to the availability, through special modems and telephone connections, of the AFGL CDC-6600. Since that time the programs have been transferred to AFGL and, while not completed, tests of the model dynamics on that machine have been undertaken. ←

The basic strategy in the modeling effort was to use the modified SCM codes to specify the large scale dynamical properties of the upper atmospheric region

and for the integration of the time dependent, three-dimensional mass continuity equations for the chemically active species. Development of the chemical and sub-scale transport properties of the model were to be undertaken by the AFGL group under the direction of Dr. S. P. Zimmerman. Thus, the complete modeling program was devised to be a cooperative venture between Georgia Tech and AFGL.

Accomplishments.

The program's goal was to create a three-dimensional model of the mesosphere and lower thermosphere over a three-year period with limited funds. The model was to incorporate simplified dynamics and interactive chemistry. A "first" run of a single simulation experiment with the completed model was anticipated late in the third year. Thus, intermediate results of a scientifically viable nature could not be expected prior to completion of the program. While the program has been cut short before these goals could be attained, substantial progress has been made, particularly in the modification of the dynamical portions of the model codes and the changes required to run the model on the AFGL CDC-6600 machine.

A. Model heating

One of the principal needs of the upper atmospheric model is the incorporation of realistic heat forcing processes for the 40-400 km regions of interest. Considerable thought, therefore, has been given to this problem.

The existing Dynamical/Chemical Stratospheric Circulation Model (SCM), which is being revised for the present work to include mesospheric and lower thermospheric levels, currently uses heating codes applicable to altitudes below ~ 80 km. Since a number of quite different physical processes lead to atmospheric heating in the thermosphere, new model codes will have to be developed for these thermospheric levels. For this, however, we must keep in mind that such codes must be considerably simplified because of time and size limitations which must be imposed on the already large three-dimensional calculations.

Some of the heating processes we have considered include:

(1) Direct solar absorption

It is convenient to divide the solar spectrum into several large wavelength segments according to their absorption characteristics and treat each of these segments separately.

a. 2050 - 3000 Å region.

Heating is due to absorption by both O_2 and O_3 in this region and is most important at the lowest thermospheric and mesospheric levels (i.e., < 100 km). Model treatment for this region can be essentially the same as was devised for the SCM (see Cunnold, et al., 1975). For example, for O_3 , the rate of temperature change due to O_3 absorption is approximated by the linear law

$$\left(\frac{\partial T}{\partial t}\right)_{O_3} = \frac{\chi_{O_3}}{M} Q(N \sec \zeta)$$

where χ_{O_3} is the number mixing ratio of O_3 , M the mass of an average air molecule, $Q(N \sec \zeta)$ the heating rate due to absorption by one molecule of O_3 , N is the number of O_3 molecules in the cm^2 vertical column above the point of heating, and ζ is the solar zenith angle. In the SCM calculations the heating rate, Q , is approximated by a finite sum over a number of small spectral intervals centered on wavelengths λ_i in the form

$$Q(N \sec \zeta) = \sum_i \alpha_{O_3}(\lambda_i) F(\lambda_i) \frac{1}{\lambda_i} \exp(-N \sec \zeta)$$

in which $\alpha_{O_3}(\lambda_i)$ is the absorption coefficient of O_3 and $F(\lambda_i)$ is the solar flux of photons integrated over each λ_i interval. In the calculations, tables of α_{O_3} , F , and the exponential functions are maintained for a wide range of likely values.

b. 1027 - 1300 Å and 1750 - 2050 Å (Schumann-Runge bands) regions.

Absorption by O_2 in these two banded regions is comparatively large below about 120 km altitude but can probably be safely neglected above this level. As in the 2050 - 3000 Å region we can estimate the heating rates by summing over the important absorption bands using band averages as tabulated by Hudson and Mahle (1972) for the 1750 - 2050 Å region (although the apparent temperature dependence of the cross sections is a complication) and by Adams (1974) for the 1027 - 1300 Å region.

c. 1300 - 1750 Å (Schumann-Runge continuum) regions.

For this O_2 absorption region, the absorption cross sections are quite consistent and we should be able to treat this region as a single band. Heating by absorption in this region is most important to total heating at levels between ~ 100 and 130 km.

d. 40 - 1027 Å (EUV) region.

Nearly all photons in this frequency range are absorbed by photoionization of N_2 , O_2 , and O which leads to very complicated ionization and photoelectric processes. These processes are particularly dominant above ~ 110 km but are replaced by heating through collisional processes above ~ 300 km. It may be possible to estimate the magnitude of the heating resulting from photon absorption in the 40 - 1027 Å region by using a simple electron density model such as that of Ching and Chiu (1973) to infer photon absorption quantities and apply a heating efficiency factor of $\sim 30 - 35\%$ (Stolarski, et al., 1975). Such a model is currently being tested.

(2) Atomic oxygen recombination and deactivation

Atomic oxygen produced at high model altitudes does not recombine (and thus release its chemical energy of recombination) above ~ 120 km. Two processes, $O + O + M \rightarrow O_2 + M$ and $O + O_2 + M \rightarrow O_3 + M$ may be important here. A simple estimate for heating by these processes may be possible by assuming (Adams, 1974) that the lifetime of an oxygen atom goes from ~ 5000 years at 150 km to ~ 2 hours at 80 km. Clearly, model vertical transports will play a large role here.

The process of deactivation of $O(^1D)$ is somewhat uncertain but potentially important to heating in the lower thermosphere. Whatever the mechanism ($O(^1D) + M \rightarrow O(^3P) + M + KE$ is the prime candidate), the reaction takes place very fast and, since there is no known large source for $O(^1D)$ at night, is confined to sunlit hours. A possible estimate for $O(^1D)$ deactivation in the model may be obtained by using the results of Adams (1974, pg. 97) with suitable adjustments for diurnal and latitudinal variations.

3. Molecular thermal conduction

The flux of heat across a horizontal surface, F_z , is usually parameterized using

$$F_z = -K \frac{\partial T}{\partial z}$$

where here K represents a thermal conduction coefficient. This is a fairly simple process to represent computationally but the selection of the proper K 's will be done in consultation with the AFGL group.

4. $15\mu CO_2$ and $62\mu O$ radiational cooling

Various authors have estimated cooling rates for these two frequencies

and the model parameterization will make use of a simplified version of one of these. The 62μ O band is particularly effective above ~ 110 km while the 15μ CO₂ band seems to dominate below that level.

5. Other heating processes

Thermal heating by the dissipation of tidal and gravity waves may be important to the thermosphere. In three dimensional models, such as we are working with here, these heat quantities will be realized through the thermal and dynamic dissipation terms built into the model equations.

Joule heating and non-thermal emissions may also play a role in total thermospheric heating but their magnitudes are usually thought to be small and will thus be neglected in the current work.

B. Model lower boundary conditions

The Stratospheric Circulation Model (SCM) has been reconfigured in its vertical structure to incorporate the region ~ 40 km - 400 km in its 26 vertical levels. As required by the model, mean global temperatures (\bar{T}) and stability quantities ($\frac{d\bar{T}}{dz} - \frac{R}{C_p} \bar{T}$) at each level were obtained from the U.S. Standard Atmosphere. The quantities will be discussed and displayed in some detail in later sections. However, we want to point out that the new Mesospheric and Lower Thermospheric Model (MTM) overlaps the height range of the SCM over the MTM's lowest six levels. Thus, it will be possible to "drive" the lower boundary of the MTM using values computed from annual runs of the SCM. To this end, a special run of the SCM for a two year integration period was performed on the machine at NASA's Ames Research Center. From these results, we have obtained for transference to AFGL:

(1) A set of lower boundary conditions for temperature (T), vertical motion (W) and ozone (χ). A complete one-year cycle of these quantities for the model's 70 horizontal degrees of freedom were collected at four-hour intervals. Thus, we have tabulated (on a computer tape) the required lower boundary conditions to drive the MTM as functions of both time and space. This involves more than 1/2 million values.

(2) Twelve sets of initial conditions, one for each month of the year, were generated by the SCM runs and tabulated on tape files. This data includes values for the model temperatures, vertical motions and ozone mixing ratios in the region of overlap between the SCM and the MTM. In addition, a set of time dependent total heating values from the SCM have been collected for the one year cycle for use in driving the MTM during early dynamical tests. These functions

will be replaced by internally derived heating quantities in the MTM's final form.

All of the data fields described in (1) and (2) have been transferred (in ASCII codes) to the AFGL 6600 disk system and are available for use in the model although some may not have been rewritten in binary form as required by the MTM input scheme.

To incorporate these lower boundary conditions, the MTM codes have been extensively rewritten and tested. Furthermore, new codes have been generated to allow for the introduction of additional minor species into the model calculation in fully predictive form (through the species continuity equations). Details of the chemical production and loss terms, however, are to be added later in cooperation with the AFGL research group.

C. Dynamical tests

A considerable problem arises in working with large, non-linear numerical models concerning the viability of the final computer codes. That is, how can one feel confident that the code is correctly performing the numerical integrations originally envisioned? Even changing a working program from machine to machine frequently introduces computational errors which cannot always be detected by simple model runs. It is necessary, therefore, to subject such model codes to rigorous testing procedures whenever the codes are modified or transported to other machines. Such a procedure was undertaken and completed for the dynamical portion of the MTM subsequent to introduction of the model changes outlined in sections A and B above. Similar checks were underway for the version transferred to the AFGL CDC 6600 at the time of the stoppage of work on the model.

Of particular concern is the performance of the non-linear terms in the dynamical sections of the MTM. We thus make use of known conservative properties of the model to test for "correctness" of solutions under various model circumstances. Some care, however, has to be taken in this procedure since it is frequently very difficult to distinguish true model or programming errors from normal numerical or machine induced inaccuracies.

One series of tests which have been completed for the MTM involves running the model with the heating, frictional dissipation and lower boundary vertical motion terms all set to zero. Thus, the quasi-geostrophic set of dynamical equations reduce to the form

$$\begin{aligned} \frac{\partial \nabla^2 \psi}{\partial t} &= -2\Omega \frac{\partial \psi}{\partial \lambda} - J(\psi, \nabla^2 \psi) - \nabla \cdot f \nabla \left(\frac{\partial \chi}{\partial p} \right) \\ \frac{\partial T'}{\partial t} &= -J(\psi, T') - \frac{\sigma}{p} \nabla^2 \chi \\ R \nabla^2 T &= \nabla \cdot f \nabla \left(\frac{\partial \psi}{\partial z} \right) \end{aligned} \quad (0.1)$$

and we can show, for example, that total energy (kinetic plus available potential) must be preserved (for details of the model, see the following sections). Table 0.1 contains the results of several runs under varying conditions. As a base case, Run "A" was computed using the normal N-cycle scheme of Lorenz (1971) with $N = 4$ and an internal time step $\delta t = 1$ hour. We see from the table that $\sim 0.06\%$ of the initial model energy has been lost after one day of computations and $\sim 0.19\%$ at the end of two days. Thus, the energy has not been preserved (which, of course, is not unexpected) and we must ascertain whether the inaccuracy is due to our numerical approximations or results from some more important physical or computational problem.

Run "B" is similar to "A" but we have removed the non-linear Jacobian terms from (0.1). For this case, the table shows that the energy conserves much better during the first two days, losing only $\sim 0.014\%$. From these results it appears that the Jacobian terms generate the major inaccuracies in the model runs but it is still not certain whether this can be attributed to model errors or to numerical approximations. One possibility would be to change the N-cycle routine from four to eight cycles per step as an attempt to generate a more accurate solution. This can be of help, particularly for the linear parts of the Jacobian calculations. Still maintaining $\delta t = 1$ hour for the internal time intervals, Run "C" repeats the calculation of "A" for $N = 8$ with no improvement

Table 0.1: Total energy as a percent of the initial total energy for days 0, 1, and 2 of test Runs "A" through "F". The conditions for each run are described below the table.

Day	Run "A"*	Run "B"*	Run "C"*	Run "D"*	Run "E"*	Run "F"*
0	100.000	100.000	100.000	100.000	100.000	100.000
1	99.943	99.993	99.942	99.999	99.478	99.299
2	99.812	99.986	99.797	99.996	99.962	99.719

* All the Runs make use of the Lorentz N-cycle time stepping scheme and, unless otherwise indicated below, the friction, heating, and lower boundary vertical motion terms are all zero. The specific conditions for each run are:

Run "A": Uses the 4-cycle scheme with internal time steps $\delta t = 1$ hour.

Run "B": Same as "A" but the non-linear Jacobian (advection) terms in (0.1) are zero.

Run "C": Same as "B" but uses 8-cycles.

Run "D": Same as "A" but $\delta t = 0.2$ hours.

Run "E": Same as "A" but the lower boundary vertical motion (w_{Bot}) is forced using the results of a Stratospheric Circulation Model (SCM) computation.

Run "F": Same as "E" but heating from the SCM computation has been added.

in the accuracy of the solutions (as seen in the table). On the other hand, when we repeat the calculation of Run "A" (4 cycle) but with internal time step intervals reduced to 12 minutes ($\delta t = 0.2$ hours), the accuracy greatly improves (Run "D") with an energy loss of only $\sim 0.004\%$ during the first two days. Clearly, the small energy losses observed over the first two days of the model test runs are due to numerical inaccuracies in the time stepping scheme rather than to coding errors in the Jacobian terms.

To get an idea of the relative importance of the numerical errors detected above, we ran two more experimental tests. The first of these was computed under the conditions of Run "A" but with the vertical motion at the lower boundary of the model introduced from the results of previous runs of the SCM. For the second test we added the computed heating values from the SCM to the lower levels of the MTM. The results, shown as Runs "E" and "F" in Table 0.1, show that the energy changes introduced by these physical terms in the model are at least as large as the uncertainties created by the numerical procedures used. Thus, reductions in the time step increments used for the model to improve the accuracy of the non-linear terms are not justified since they would be masked by the forcing and boundary terms.

1. Basic dynamical equations and coordinate system.

The horizontal coordinate system will be longitude (positive eastward) and latitude, denoted by λ and ϕ . This dependence will be represented in spherical surface harmonics, except that certain terms, such as part of the heating and photochemistry will be evaluated point-wise at selected values of λ and ϕ . In the vertical direction pressure (p) will be used as a coordinate with finite-differences being employed. These pressure levels will be distributed at equal intervals of $\log P$ in order to give roughly equal intervals in height. We define

$$\left. \begin{aligned} P &= p \div (100 \text{ cbar}) \\ Z &= -\ln P, \quad P = e^{-Z} \end{aligned} \right\} . \quad (1.1)$$

From the hydrostatic relation $dp = -\rho g dz$ and $\rho = p/RT$, we have

$$dZ = -\frac{dp}{p} = \frac{g}{RT} dz \quad (1.2)$$

The vertical levels will be separated by a uniform value of ∇Z . To the extent that the temperature T is approximately uniform at near surface values, a change of one in Z corresponds to a height change of the order of 7 km. The bottom of the atmosphere, but not necessarily of the model, will, for simplicity, be taken at $Z = 0$, i.e., at $p = 100$ cb instead of at the conventional sea-level pressure of 101.325 cb.

The dynamical system not only assumes hydrostatic balance, but also a "quasi-geostrophic balance" in the horizontal equations of motion. Because we must consider global processes over the entire sphere, this balance must allow for complete variability of the Coriolis parameter f :

$$\begin{aligned}
 f &= 2\Omega \sin\phi \\
 \Omega &= 7.292 \times 10^{-5} \text{ rad sec}^{-1}
 \end{aligned}
 \tag{1.3}$$

The quasi-geostrophic balance in question is obtained as follows (Lorenz, Tellus, 1960, P. 364). First, we divide the horizontal velocity \vec{v} into a non-divergent part $\hat{k} \times \nabla\psi$ given by a stream function ψ and a divergent part $-\nabla\chi$, given by a velocity potential χ :

$$\vec{v} = \hat{k} \times \nabla\psi - \nabla\chi
 \tag{1.4}$$

If the eastward and northward components of \vec{v} are represented by u and v and a is the radius of the earth, this is equivalent to

$$\left.
 \begin{aligned}
 u &= a \cos\phi \frac{d\lambda}{dt} = -\frac{1}{a} \frac{\partial\psi}{\partial\phi} - \frac{1}{a \cos\phi} \frac{\partial\chi}{\partial\lambda} \\
 v &= a \frac{d\phi}{dt} = \frac{1}{a \cos\phi} \frac{\partial\psi}{\partial\lambda} - \frac{1}{a} \frac{\partial\chi}{\partial\phi}
 \end{aligned}
 \right\}
 \tag{1.5}$$

The vertical component of relative vorticity, ζ , and the horizontal divergence of \vec{v} are related to ψ and χ by

$$\zeta = \hat{k} \cdot \text{curl } \vec{v} = \nabla^2\psi; \quad \text{div } \vec{v} = -\nabla^2\chi
 \tag{1.6}$$

where ∇^2 is the horizontal Laplacian operator on the sphere.

The condition of the quasi-geostrophic balance is

$$\nabla \cdot f\nabla\psi = g\nabla^2z
 \tag{1.7}$$

where g is gravity and z is the height of a constant pressure surface. [Unless noted otherwise, all partial derivatives with respect to λ , ϕ , and t (time) are

carried out at constant pressure (or Z)]. The hydrostatic relation,

$$g \frac{\partial z}{\partial p} = - \frac{1}{\rho} = - \frac{RT}{p} \quad (1.8a)$$

or

$$g \frac{\partial z}{\partial Z} = RT \quad (1.8b)$$

enables (1.7) to be rewritten as

$$\nabla \cdot f \nabla \frac{\partial \psi}{\partial Z} = \nabla^2 RT \quad (1.9)$$

Associated with this relation (which is a simplified form of the equation obtained by taking the horizontal divergence of the equations of motion) is the "vorticity equation":

$$\nabla^2 \frac{\partial \psi}{\partial t} = - \hat{k} \times \nabla \psi \cdot \nabla (f + \nabla^2 \psi) + \nabla \cdot f \nabla \chi + \nabla \cdot (\vec{F}_r \times \hat{k}) \quad (1.10)$$

where \vec{F}_r is the horizontal frictional force per unit mass.

The continuity equation (conservation of mass) is

$$\frac{\partial}{\partial p} \left(\frac{dp}{dt} \right) = \frac{\partial}{\partial p} \left(\frac{dP}{dt} \right) = -\nabla \cdot \vec{v} = \nabla^2 \chi \quad (1.11)$$

The upper boundary condition at $Z = Z_{\text{top}}$ will be that dp/dt vanishes there. Let us define

$$\chi = - \int_{p_{\text{top}}}^p \chi dp, \quad \chi = - \frac{\partial \chi}{\partial p} \quad (1.12)$$

Equation (1.10) can then be rewritten as

$$\nabla^2 \frac{\partial \psi}{\partial t} = - \hat{k} \times \nabla \psi \cdot \nabla (f + \nabla^2 \psi) - \nabla \cdot f \nabla \left(\frac{\partial \chi}{\partial p} \right) + \nabla \cdot (\vec{F} r x \hat{k}) \quad (1.13)$$

If we use $Z = -\ln P$ as the vertical coordinate, the appropriate vertical advection velocity is

$$W = \frac{dZ}{dt} = - \frac{1}{P} \frac{dP}{dt} \quad (1.14)$$

The continuity equation (1.11) in terms of W is:

$$\nabla \cdot P \vec{V} + \partial(PW) / \partial Z = 0 \quad (1.15)$$

From (1.11), (1.12) and (1.14) we get $\partial[PW - \nabla^2 \chi] / \partial P = 0$, or

$$PW = \nabla^2 \chi \quad (1.16)$$

Boundary conditions on W are that W vanishes at Z_{top} and that it is given from external sources at the bottom:

$$Z = Z_{top}: W = 0 \quad (1.17)$$

$$Z = Z_{bot}: W = W_0(t, \lambda, \phi) \text{ as given.} \quad (1.17a)$$

Since Z_{bot} is some distance above the actual earth's surface, we must also specify the bottom dynamical and thermodynamical conditions. For this purpose, we will make use of previous runs of the model version which includes the surface as its bottom boundary. The results from such a computation will be used to specify the bottom boundary temperature field (in space and time) for the present upper level model. Thus, we have

$$Z = Z_{bot}: T = T_0(t, \lambda, \phi) \text{ as given.} \quad (1.17b)$$

The bottom streamfunction field will then be given through the thermal wind equation.

Friction will be represented by a vertical Austausch, $\vec{F}_r = \frac{1}{\rho} \frac{\partial \vec{\tau}}{\partial z} = -g \frac{\partial \vec{\tau}}{\partial p}$. Thus $\nabla \cdot \vec{F}_r \hat{k} = \frac{\partial}{\partial p} [\nabla \cdot (\frac{-g \vec{\tau}}{p_0} \hat{k})]$. We set $\vec{\tau} = \rho K_m \partial(\hat{k} \times \nabla \psi) / \partial z$, giving

$$\nabla \cdot (\frac{-g \vec{\tau}}{p_0} \hat{k}) = \nabla \cdot [\frac{g^2 \rho^2}{p_0^2} K_m \frac{\partial \nabla \psi}{\partial p}]$$

Using the "scale height"

$$H_0 = \frac{RT_0}{g}, \quad (1.18)$$

replacing ρ by p/RT and replacing g/RT by $1/H_0$ we get

$$\nabla \cdot (\frac{-g \vec{\tau}}{p_0} \hat{k}) = -\frac{K_m}{H_0^2} p \frac{\partial \nabla^2 \psi}{\partial z}$$

To summarize the friction term we can write

$$\left. \begin{aligned} \nabla \cdot \vec{F}_r \hat{k} &= \frac{\partial}{\partial p} (PF) \\ z > 0: F &= \frac{K_m}{H_0^2} p \frac{\partial \nabla^2 \psi}{\partial z} \end{aligned} \right\} \quad (1.19)$$

At $Z = Z_{top}$, F will vanish (no stress).

The next physical statement is the thermodynamic law $d(\text{entropy})/dt =$ rate of heating \div temperature. For our perfect gas system this would be

$$C_p \frac{d}{dt} [\ln(T p^{-\kappa})] = \frac{q}{T}; \quad \kappa = \frac{R}{C_p} = \frac{2}{7} \quad (1.20)$$

where q is the rate of heating per unit mass and T the temperature. In terms

of T, this becomes

$$\frac{\partial T}{\partial t} = -(\hat{k}_x \nabla \psi - \nabla \chi) \cdot \nabla T - W \frac{\partial T}{\partial Z} - \kappa W T + \frac{q}{C_p} \quad (1.21)$$

We will, however, use a simplified form of this, obtained by ignoring $\nabla \psi \cdot \nabla T$ and by replacing T in $W \partial T / \partial Z$ and $\kappa W T$ by \bar{T} , where \bar{T} is the horizontal average:

$$\left. \begin{aligned} T &= \bar{T}(p, t) + T'(\lambda, \phi, p, t) \\ \bar{T} &= \frac{1}{4\pi a^2} \int_{-\pi/2}^{\pi/2} \cos \phi d\phi \int_0^{2\pi} T d\lambda; \quad \bar{T}' = 0 \end{aligned} \right\} \quad (1.22)$$

[This definition of $(\bar{\quad})$ and $(\quad)'$ will be applicable to any variable.] This greatly simplifies the computations, and is reasonably accurate because $\nabla \psi \gg \nabla \chi$ and $\partial T' / \partial Z + \kappa T'$ is generally small compared to $\partial \bar{T} / \partial Z + \kappa \bar{T}$. The result is

$$\frac{\partial \bar{T}}{\partial t} = -\hat{k}_x \nabla \psi \cdot \nabla T - W \left(\frac{d\bar{T}}{dZ} + \kappa \bar{T} \right) + q / C_p \quad (1.23)$$

However, this simplification has the result that we can no longer interpret (1.23) as forecasting \bar{T} , the horizontally averaged T; this is because the horizontal average of (1.23) gives simply

$$\frac{\partial \bar{T}}{\partial t} = \bar{q} / C_p$$

whereas the horizontal average of the exact equation (1.21) gives

$$\frac{\partial \bar{T}}{\partial t} = \frac{\bar{q}}{C_p} - \kappa \overline{W T'} - \frac{1}{p} \frac{\partial}{\partial Z} (p \overline{W T'}), \quad (1.24)$$

showing the effect of vertical transports of entropy by the motion. We expect little change in \bar{T} from the observed annual average $\bar{T}(Z)$, however, either with season or with changes in the ozone chemistry. [The effect of the latter will be discussed separately.]

In passing, we note that

$$\begin{aligned} \frac{\partial T}{\partial Z} + \kappa T &= \frac{RT}{g} \left(\frac{\partial T}{\partial Z} + \frac{g}{C_p} \right) \\ &= T \frac{\partial}{\partial Z} [\ln(T p^{-\kappa})] \\ &= \frac{N^2}{R} \left(\frac{RT}{g} \right)^2 \end{aligned} \quad (1.25)$$

where N is the buoyancy frequency.

Finally, we describe the basic form of the equation for the (number density) mixing ratio of a trace substance such as O_3 . Define

$$x_i = n_i / n_m \quad (1.26)$$

where n_i is the number density of the i -th trace substance, n_m is the total number density. For levels below ~ 110 km we use

$$\begin{aligned} n_m &\cong p/kT \\ k &= \text{Boltzman constant} = 1.380 \times 10^{-26} \text{ kilojoules deg}^{-1} \end{aligned} \quad (1.27)$$

Above ~ 110 km, $n_m = \sum_i n_i$.

The equation for $d x_i / dt$ (the rate of change following the motion) is

$$\begin{aligned} \frac{dX_i}{dt} &= \frac{\partial X_i}{\partial t} + (\hat{k} \times \nabla \psi - \nabla \chi) \cdot \nabla X_i + W \frac{\partial X_i}{\partial Z} \\ &= \frac{1}{n_m} \left(\frac{dn_i}{dt} \right)_c + \frac{1}{p} \frac{\partial}{\partial Z} \left[\rho K_d \frac{\partial X_i}{\partial Z} \right] \end{aligned}$$

where $(dn_i/dt)_c$ is the net rate of local photochemical generation of the substance (number per unit volume per unit time) and K_d is the vertical eddy-diffusion coefficient [with dimensions $\text{length}^2 \div \text{time}$]. K_d will vary only with P .

The vertical diffusion term can be rewritten by using the hydrostatic equation as

$$\frac{\partial}{\partial P} \left[K_d \left(\frac{gP}{RT} \right)^2 \frac{\partial X_i}{\partial P} \right] = \frac{\partial}{\partial P} \left[- \frac{K_d}{H_0^2} P \frac{\partial X_i}{\partial Z} \right] \quad (1.28)$$

where we have again absorbed the variation of density with T into H_0 on the recognition that K_d itself is not a precisely known quantity. K_d (and the momentum Austausch K_m) will be prescribed functions of P . The equation for X_i is now

$$\frac{\partial X_i}{\partial t} = -(\hat{k} \times \nabla \psi - \nabla \chi) \cdot \nabla X_i - W \frac{\partial X_i}{\partial Z} + \frac{1}{n_m} \left(\frac{dn_i}{dt} \right)_c + \frac{\partial}{\partial P} \left[- \frac{K_d}{H_0^2} P \frac{\partial X_i}{\partial Z} \right] \quad (1.29)$$

or

$$\begin{aligned} \frac{\partial X_i}{\partial t} &= - \frac{1}{P} \left[\nabla \cdot (P \vec{v} X_i) + \frac{\partial (P W X_i)}{\partial Z} \right] \\ &\quad + \frac{1}{n_m} \left(\frac{dn_i}{dt} \right)_c + \frac{\partial}{\partial P} \left[- \frac{K_d}{H_0^2} P \frac{\partial X_i}{\partial Z} \right] \end{aligned} \quad (1.30)$$

[having made use of (1.4) and (1.15) to obtain the last form].

The rate of change of $\bar{\chi}_i$ (the horizontal average) is obtained from the horizontal average of (1.30):

$$\frac{\partial \bar{\chi}_i}{\partial t} = \frac{\partial}{\partial P} [P \bar{w} \chi_i] + \left[\frac{1}{n_m} \left(\frac{dn_i}{dt} \right)_c \right] + \frac{\partial}{\partial P} \left[- \frac{K_d}{H_0^2} P \frac{\partial \bar{\chi}_i}{\partial Z} \right] \quad (1.31)$$

The rate of change of χ_i' will, however, be obtained from a simplified form of (1.29), much as was done in the thermodynamic equation (1.23):

$$\begin{aligned} \frac{\partial \chi_i'}{\partial t} = & - \hat{k}_x \nabla \psi \cdot \nabla \chi_i' - w \frac{\partial \chi_i'}{\partial Z} \\ & + \left[\frac{1}{n_m} \frac{dn_i}{dt} \right]'_c + \frac{\partial}{\partial P} \left[- \frac{K_d}{H_0^2} P \frac{\partial \chi_i'}{\partial Z} \right] \end{aligned} \quad (1.32)$$

In contrast to \bar{T} , where we are for the most part content to take \bar{T} as given, we must predict $\bar{\chi}_i$ as well as χ_i' . Equation (1.31) will therefore be used as well as (1.32).

Presumably (1.33) need not be applied every time step in the numerical integration, $\bar{\chi}_i$ being a slowly changing function of time. However, the term $\bar{w} \chi_i$ must be put equal to zero at $P = 1$ to ensure no net creation of χ_i by the large scale motion.

A special treatment of the minor species equation will be necessary at certain levels. As an example, Lindzen and Goody (J. Atmos. Sci., 1965, P. 341) show that the photodissociation of ozone is extremely rapid at heights above 45 km, with a time constant becoming less than 1 hour. (They presumably use typical values of incident solar radiation). The conventional methods of "time-

stepping) equations such as (1.32) require a computational time step no longer than the characteristic physical times associated with terms on the right side of (1.32). Since the advective time scale is of the order of an hour or so, we must consider replacing (1.31) and (1.32) at these levels by the equilibrium condition.

$$x_i = (x_i)_{\text{equil}} \Leftrightarrow \frac{dn_i}{dt} = 0 \quad (1.33)$$

2. Choice of vertical levels.

We obtain equal intervals in $Z = -\ell \ln P$ ($P =$ pressure : 100 cb) by defining

$$\left. \begin{aligned} Z_j &= \Delta Z(J-j) \\ P_j &= e^{-\Delta Z(J-j)} \end{aligned} \right\} J = 1, 2, \dots, J. \quad (2.1)$$

$j = 1$ is at the "top" of our model atmosphere, and $j = J$ at the bottom, whence

$$Z = \frac{Z_1}{J-1} = \frac{Z_{\text{top}}}{J-1} .$$

A convenient choice is obtained by choosing

$$\begin{aligned} e^{\Delta Z} &= r, \quad r = 2.12472 \\ \Delta Z &= \ell nr = 0.753640 \end{aligned} \quad (2.2)$$

so that

$$\begin{aligned} Z_1 &= Z_{\text{top}} = (J-1)\ell nr \\ P_1 &= r^{-(J-1)} \end{aligned} \quad (2.3)$$

Successive pressure levels are separated by (roughly) 6 km below the turbopause. The relations

$$P_j = r^{-(J-j)}; \quad P_{j+1} = rP_j \quad (2.4)$$

are useful. At these levels, the following basic variables will be represented $j = 1, 2, \dots, J$: $T_j, W_j, (X_i)_j$ together with the heating rate, the photochemical term, and the vertical turbulent fluxes of momentum. At the intermediate levels

the streamfunction ψ_j will be represented

$$j = \frac{3}{2}, \frac{5}{2}, \dots, J - \frac{1}{2} : \psi_j$$

For convenience in notation, however, ψ will be labeled with an interger subscript according to the convention

$$\psi(P = P_{j+1/2}) = \psi_j$$

This results in the scheme as seen in Figure 2.1.

Table 2.1 lists the values of the more basic variables for the choice $r = 2.12472$, $J = 26$. Values of \bar{T} were taken from the U.S. Standard Atmosphere, 1976 (NOAA, NASA, and USAF). The static stability parameter S is defined later in equation (3.20).

Figure 2.1: Vertical levels of the model and the location on these levels of the model variables.

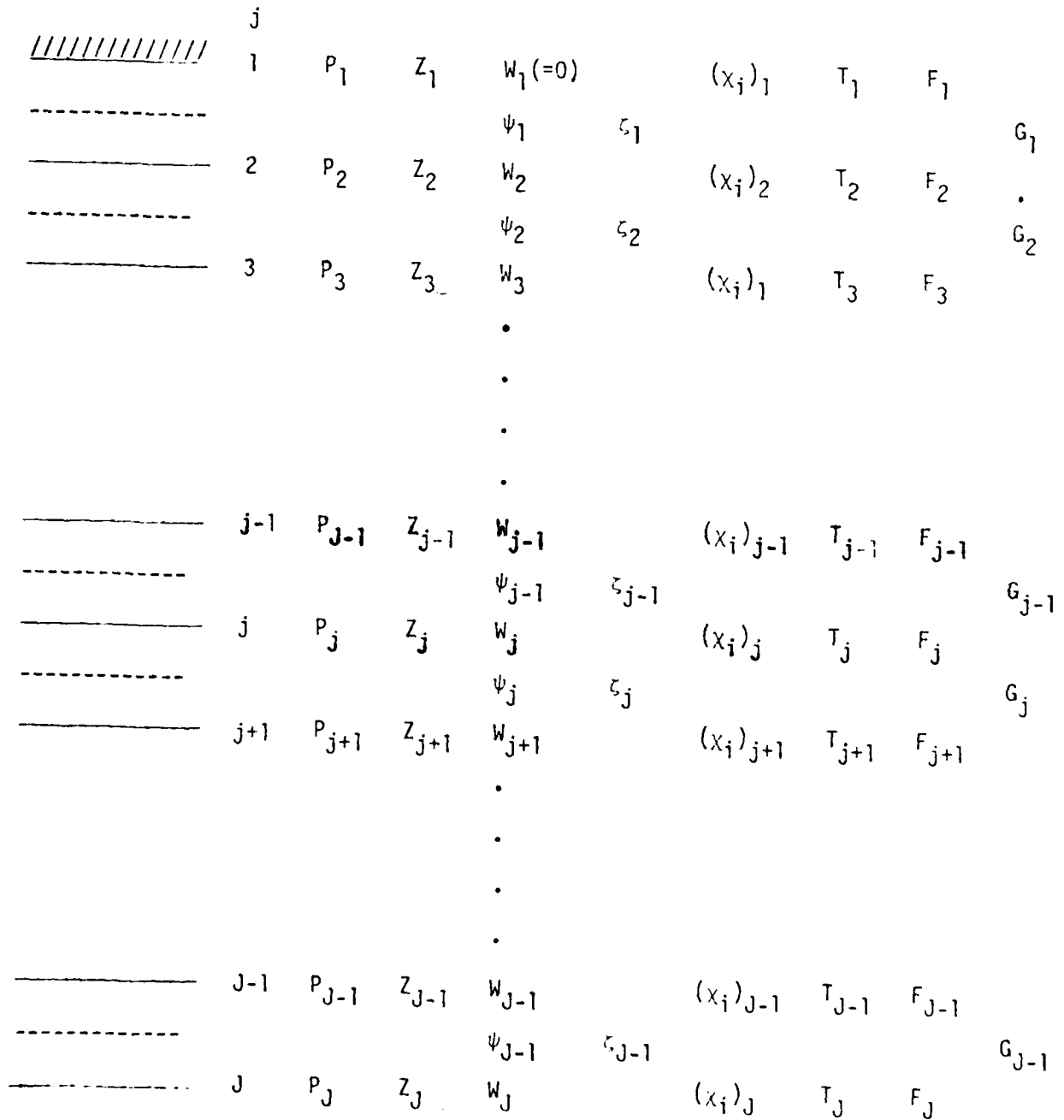


TABLE 2.1

Pressure, temperature, approximate height,
and static stability for model levels.

Level	Z (= $-\ln(p/1000\text{mb})$)	$p(\text{mb})$	$\bar{T}(\text{°k})$	$z(\text{km})$	$\frac{d\bar{T}}{dz} + \frac{R}{c_p}\bar{T}(\text{°k})$
1	24.92	0.15 (-7)	995.5	398.0	289.01
2	24.17	0.32 (-7)	991.0	354.3	292.70
3	23.42	0.68 (-7)	981.0	313.6	299.13
4	22.66	0.14 (-6)	962.5	275.2	308.45
5	21.91	0.31 (-6)	930.5	240.7	321.53
6	21.15	0.65 (-6)	878.5	210.0	336.53
7	20.40	0.14 (-5)	801.5	183.1	346.05
8	19.65	0.29 (-5)	702.0	161.0	345.16
9	18.89	0.62 (-5)	583.5	143.0	327.56
10	18.14	0.13 (-4)	459.5	129.0	288.16
11	17.39	0.28 (-4)	347.0	118.9	233.47
12	16.63	0.60 (-4)	257.0	111.4	162.65
13	15.88	0.13 (-3)	212.5	106.0	100.51
14	15.13	0.27 (-3)	197.0	101.0	71.20
15	14.37	0.57 (-3)	190.0	96.6	60.91
16	13.62	0.12 (-2)	187.0	92.3	55.41
17	12.86	0.26 (-2)	187.0	88.0	50.76
18	12.11	0.55 (-2)	191.0	83.9	45.93
19	11.36	0.01	200.0	79.5	45.52
20	10.60	0.02	208.5	74.8	46.62

21	9.85	0.05	219.5	69.8	47.77
22	9.10	0.11	231.0	64.7	49.07
23	8.34	0.24	245.0	59.3	50.08
24	7.59	0.51	261.0	53.7	59.96
25	6.84	1.07	267.0	47.8	80.58
26	6.08	2.28	254.5	41.9	88.62

Note: Levels 21-26 (between the dashed lines) are levels which overlap the Stratospheric Circulation Model.

3. Non-dimensional finite-difference equations

In this section we write the basic equations in a non-dimensional form (primarily to simplify the dynamical computations) and simultaneously introduce the vertical finite-difference representation defined in Section 2. We define

$$\begin{aligned}\mu &= \sin\phi \\ \nabla(\text{dim}) &= \frac{1}{a} \nabla(\text{non-dim}) \\ \nabla^2(\text{dim}) &= \frac{1}{a^2} \nabla^2(\text{non-dim}) \\ \psi(\text{dim}) &= 2\Omega a^2 \psi(\text{non-dim}) \\ X(\text{dim}) &= 2\Omega a^2 X(\text{non-dim}) \\ t(\text{dim}) &= \frac{1}{2\Omega} t(\text{non-dim}) \\ W(\text{dim}) &= 2\Omega W(\text{non-dim}) \\ T(\text{dim}) &= (4\Omega^2 a^2/R) \bar{T}(\text{non-dim}) + (4\Omega^2 a^2/R) T(\text{non-dim})\end{aligned}\tag{3.1}$$

In the last expression $T(\text{dim})$ is the "total" temperature in absolute degrees, $\bar{T} = \bar{T}(Z)$ is the "standard atmosphere" temperature (also in degrees) given in the table at the end of Section 2, while the quantity $(4\Omega^2 a^2/R) T(\text{non-dim})$ is the (deviation from the horizontal mean) variable T appearing in (1.23), having a zero horizontal average. [The total $T(\text{dim})$ is, of course, used in all chemical computations].

$$\begin{aligned}\Omega &= 2\pi/8.64 \times 10^4 \text{ rad sec}^{-1} \\ a &= 6.371 \times 10^6 \text{ meters} \\ R &= 287 \text{ kJ ton}^{-1} \text{ deg}^{-1} \\ C_p &= (7/2)R\end{aligned}\tag{3.2}$$

One day, $(2\pi/\Omega)$ secs, corresponds to

$$\Delta t(\text{non-dim}) = 2\Omega \left(\frac{2\pi}{\Omega} \right) = 4\pi \quad (3.3)$$

The non-dimensional ∇^2 operator is

$$\nabla^2(\) = \frac{1}{\cos^2 \phi} \frac{\partial^2(\)}{\partial \lambda^2} + \frac{1}{\cos \phi} \frac{\partial}{\partial \phi} \left[\cos \phi \frac{\partial(\)}{\partial \phi} \right] \quad (3.4)$$

The relation

$$PW = \nabla^2 X \quad (3.16)$$

between W and X can be used to eliminate X in favor of W [in equation (1.13)],

by defining the inverse Laplacian operator

$$\left. \begin{aligned} L &\equiv \nabla^{-2} \\ X &= PLW \end{aligned} \right\} \quad (3.5)$$

We also have

$$\zeta = \nabla^2 \psi; \quad \psi = L\zeta \quad (3.6)$$

A further convenient arrangement is useful for evaluating terms of the form $\partial(PF)/\partial P$, which appears in the vertical diffusion terms for vorticity and trace substances and in the term

$$\frac{\partial X}{\partial P} = \frac{\partial}{\partial P} [P(LW)]$$

in the vorticity equation (1.13). We have

$$\left[\frac{\partial}{\partial P} (PF) \right]_j = \frac{P_{j+1/2} F_{j+1/2} - P_{j-1/2} F_{j-1/2}}{P_{j+1/2} - P_{j-1/2}} = \left(\frac{r}{r-1} \right) F_{j+1/2} - \left(\frac{1}{r-1} \right) F_{j-1/2} \quad (3.7)$$

where we have made use of (2.4).

The horizontal advection of a quantity F can be written as the Jacobian

$$\begin{aligned} -\vec{v}_\psi \cdot \nabla F &= -\hat{k} \times \nabla \psi \cdot \nabla F = \frac{\partial F}{\partial \lambda} \frac{\partial \psi}{\partial \mu} - \frac{\partial \psi}{\partial \lambda} \frac{\partial F}{\partial \mu} \\ &\equiv J(F, \psi) \end{aligned} \quad (3.8)$$

The non-dimensional form of the vorticity equation (1.13), with regard to the subscript labelling defined in Section 2, together with equation (1.19) and (3.5) - (3.8) is as follows:

For $j = 1, 2, \dots, J-1$:

$$\begin{aligned} \frac{\partial \zeta_j}{\partial t} &= J(\mu + \zeta_j, \psi_j) - \nabla \cdot \{ \mu \nabla L [(\frac{r}{r-1}) W_{j+1} - (\frac{1}{r-1}) W_j] + \\ &\quad + (\frac{r}{r-1}) F_{j+1} - (\frac{1}{r-1}) F_j \} \end{aligned} \quad (3.9)$$

$$\psi_j = L \zeta_j \quad (3.10)$$

$$F_1 = 0 \quad (3.11)$$

$$F_J = -D \zeta_{J-1} \quad (3.12)$$

$$F_j = E_j (\zeta_j - \zeta_{j-1}) \quad (j = 2, 3, \dots, J-1) \quad (3.13)$$

$$E_j = (K_m)_j \div [H_0^2 2\Omega \Delta Z] \quad (3.14)$$

$$D = k_D \div 2\Omega \quad (3.15)$$

$$W_1 = 0 \quad (3.16)$$

$$W_J = -J(\frac{h}{H_0}, \psi_{J-1}) \quad (3.17)$$

The non-dimensional form of the "thermal wind equation" (1.9) becomes for

$$j = 2, 3, \dots, J-1:$$

$$V \cdot \nabla (\psi_j - \psi_{j-1}) = -V^2 T_j \Delta Z \quad (3.18)$$

The non-dimensional form of the thermal equation (1.23) becomes for

$$j = 2, 3, \dots, J-1:$$

$$\frac{\partial T_j}{\partial t} = \frac{1}{2} J(T_j, \psi_j + \psi_{j-1}) - S_j W_j + \left[\frac{R}{C_p 2\Omega^2 a^2} \right] q_j \quad (3.19)$$

where

$$S_j = \left(\frac{R}{4\Omega^2 a^2} \right) \left[\frac{dT}{dZ} + \frac{R}{C_p} T \right]_j \quad (3.20)$$

is tabulated at the end of Section 2. Note that q_j , the rate of heating per unit mass, is still in dimensional form in (3.19).

The trace substance is, for

$$j = j_0, j_0+1, \dots, J-1:$$

$$\begin{aligned} \frac{\partial x_j}{\partial t} = & \frac{1}{2} J(x_j, \psi_j + \psi_{j-1}) - w_j \left(\frac{d\zeta}{dz} \right) + \left(\frac{r}{r-1} \right) G_j - \left(\frac{1}{r-1} \right) G_{j-1} + \\ & + \left(\frac{1}{2\Omega} \right) \left[\frac{1}{n_m} \left(\frac{dn}{dt} \right)_c \right]_j \end{aligned} \quad (3.21)$$

$$G_j = D_j (x_{j+1} - x_j) ; \quad \text{for } j=j_0, \dots, J-2$$

$$D_j = (K_d)_{j+1/2} : (2\Omega H_0^2 \Delta Z) \quad (3.22)$$

[The vertical diffusion coefficient K_d is defined at the Z_j -levels corresponding

to $j = \text{integer plus } 1/2$, whereas the vertical exchange coefficient K_m for vorticity, appearing in (3.14), is defined at integer values of j .]

4. Spectral form of the equations

We define spectral solutions at arbitrary level j in the form

$$\left. \begin{aligned} \psi_j &= \sum_{\alpha} \psi_{\alpha,j} Y_{\alpha}(\lambda, \mu) \\ \zeta_j &= \sum_{\alpha} \zeta_{\alpha,j} Y_{\alpha}(\lambda, \mu) \\ W_j &= \sum_{\alpha} W_{\alpha,j} Y_{\alpha}(\lambda, \mu) \\ T_j &= \sum_{\alpha} T_{\alpha,j} Y_{\alpha}(\lambda, \mu) \\ q_j &= \sum_{\alpha} q_{\alpha,j} Y_{\alpha}(\lambda, \mu) \end{aligned} \right\} \quad (4.1)$$

and for the trace substance equation

$$\left. \begin{aligned} X_j &= \sum_{\alpha} X_{\alpha,j} Y_{\alpha}(\lambda, \mu) \\ G_j &= \sum_{\alpha} G_{\alpha,j} Y_{\alpha}(\lambda, \mu) \end{aligned} \right\} \quad (4.2)$$

In terms of longitude (λ) and latitude (μ), we have defined members of the complete set of orthogonal spherical harmonics in (4.1) and (4.2) using

$$Y_{\alpha}(\lambda, \mu) = e^{i\ell_{\alpha}\lambda} P_{\alpha}(\mu) \quad (4.3)$$

with

$$\alpha = n_{\alpha} + i\ell_{\alpha} \quad (4.4)$$

denoting a vector index of planetary wave number ℓ_{α} and degree n_{α} . The $P_{\alpha}(\mu)$ are Legendre polynomials of rank and degree given by α . Normalization of the

spherical harmonics is such that integration over the unit spherical surface (s) yields the orthogonal property

$$\int_S Y_\alpha Y_\beta^* ds = 4\pi \delta_{\alpha,\beta} \quad (4.5)$$

Complex conjugate values are denoted by an asterisk. Another useful property of the set of spherical harmonics is that they satisfy the differential equation

$$\nabla^2 Y_\alpha = -c_\alpha Y_\alpha; \quad c_\alpha = n_\alpha(n_\alpha + 1) \quad (4.6)$$

The complete set of orthonormal Legendre polynomials as used in (4.3) are defined such that

$$P_\alpha^* \equiv P_\alpha \quad (4.7)$$

and all P_α have been normalized such that

$$\int_{-1}^{+1} P_\alpha P_\beta d\mu = 2\delta_{\alpha,\beta} \quad (4.8)$$

We now want to substitute solutions (4.1) and (4.2) into the non-dimensional forms of our model equations, multiply through with a member of the orthogonal set (say, Y_γ^*), and integrate the resulting relationships over the unit sphere. Application of this procedure to the vorticity equation (3.9), for example, yields the desired spectral form of this equation,

$$\begin{aligned}
\frac{dr_{Y,j}}{dt} = & -i\ell_Y \psi_{Y,j} - A_{Y,j} + \frac{D_Y}{c_{Y-\varepsilon}} \left[\left(\frac{r}{r-1}\right) W_{Y-\varepsilon,j+1} - \right. \\
& \left. - \left(\frac{1}{r-1}\right) W_{Y-\varepsilon,j} \right] - \frac{E_Y}{c_{Y+\varepsilon}} \left[\left(\frac{r}{r-1}\right) W_{Y+\varepsilon,j+1} - \right. \\
& \left. - \left(\frac{1}{r-1}\right) W_{Y+\varepsilon,j} \right] + \left(\frac{r}{r-1}\right) F_{Y,j+1} - \left(\frac{1}{r-1}\right) F_{Y,j}
\end{aligned} \tag{4.9}$$

in which, over the unit spherical surface s ,

$$\begin{aligned}
\frac{dr_{Y,j}}{dt} &= \frac{1}{4\pi} \int_S \frac{\partial r_j}{\partial t} Y_Y^* ds \\
i\ell_Y \psi_{Y,j} &= \frac{1}{4\pi} \int_S J(\psi_j, \mu) Y_Y^* ds = \frac{1}{4\pi} \int_S \frac{\partial \psi_j}{\partial \lambda} Y_Y^* ds \\
A_{Y,j} &= \frac{1}{4\pi} \int_S J(\psi_j, \zeta_j) Y_Y^* ds \quad (\text{See Appendix A}) \\
\frac{D_Y}{c_{Y-\varepsilon}} W_{Y-\varepsilon,j} - \frac{E_Y}{c_{Y+\varepsilon}} W_{Y+\varepsilon,j} &= -\frac{1}{4\pi} \int_S [\nabla \cdot \mu \nabla L(W_j)] Y_Y^* ds \quad (\text{See Appendix B}) \\
F_{Y,j} &= \frac{1}{4\pi} \int_S F_j Y_Y^* ds
\end{aligned} \tag{4.10}$$

Similarly, the thermodynamic energy equation (3.19), the trace substance equation (3.21), and the thermal wind relationship (3.18) reduce to the spectral forms

$$\begin{aligned}
 \frac{dT_{Y,j}}{dt} &= -B_{Y,j} - S_j W_{Y,j} + \left[\frac{R}{C_p 3\Omega^2 a^2} \right] q_{Y,j} \\
 \frac{d\chi_{Y,j}}{dt} &= -B_{Y,j}^{(\chi)} - \left(\frac{d\bar{\chi}}{dz} \right) W_{Y,j} + \left(\frac{r}{r-1} \right) G_{Y,j} - \\
 &\quad - \left(\frac{1}{r-1} \right) G_{Y,j-1} + \frac{1}{4\pi} \int_S \frac{1}{2\Omega} \left[\frac{1}{n_m} \left(\frac{dn}{dt} \right) c \right]_j Y_Y^* ds \\
 \Delta Z c_{Y,j} T_{Y,j} &= -D_Y (\psi_{Y-\epsilon,j-1} - \psi_{Y-\epsilon,j}) + E (\psi_{Y+\epsilon,j-1} - \psi_{Y+\epsilon,j})
 \end{aligned} \tag{4.11}$$

where, for example,

$$\begin{aligned}
 \frac{dT_{Y,j}}{dt} &= \frac{1}{4\pi} \int_S \frac{\partial T_j}{\partial t} Y_Y^* ds \\
 \frac{d\chi_{Y,j}}{dt} &= 4\pi \int_S \frac{d\chi_j}{dt} Y_Y^* ds \\
 c_{Y,j} T_{Y,j} &= \frac{1}{4\pi} \int_S (-\nabla^2 T_j) Y_Y^* ds \\
 B_{Y,j} &= \frac{1}{8\pi} \int_S J(\psi_j + \psi_{j-1}, T_j) Y_Y^* ds \quad (\text{See Appendix A}) \\
 B_{Y,j}^{(\chi)} &= \frac{1}{8\pi} \int_S J(\psi_j + \psi_{j-1}, \chi_j) Y_Y^* ds \quad (\text{See Appendix A}) \\
 D_Y \psi_{Y-\epsilon,j} - E_Y \psi_{Y+\epsilon,j} &= -\frac{1}{4\pi} \int_S [\nabla \cdot \mu \nabla \psi_j] Y_Y^* ds \quad (\text{See Appendix B})
 \end{aligned} \tag{4.12}$$

In addition, we want to determine the spectral form of (1.6) relating the verti-

cal component of relative vorticity (ζ) and the streamfunction (ψ). It can be shown that

$$\zeta_{\gamma,j} = -c_{\gamma}\psi_{\gamma,j} \quad (4.13)$$

or

$$\psi_{\gamma,j} = -\frac{\zeta_{\gamma,j}}{c_{\gamma}} \quad (4.14)$$

provided that in (6.14) we stipulate $\gamma \neq 0 + i0$ (i.e., $c_{\gamma} \neq 0$).

The spectral relationships (4.9), (4.11), and (4.13) [or (4.14)] along with definitions (4.10) and (4.12) form a complete set of equations for solution. However, it is not convenient to attempt to integrate the model in this form as there is no explicit relationship determining the vertical velocity field represented by W . In order to define W , we want to alter the thermal wind relationship in (4.11). This development is contained in the next section. Furthermore, specification of the truncation limits to be used for series solutions (4.1) and (4.2) have not yet been established and will be discussed in a later section.

5. Determination of W in the dynamic equations

In order to obtain an explicit description of the vertical motion fields in our model atmosphere, we insert (4.14) into the thermal wind equation of (4.11) and differentiate w.r.t. time to get

$$\Delta Z c_{\gamma} \frac{dT_{\gamma,j}}{dt} = \frac{D_{\gamma}}{c_{\gamma-\epsilon}} \left(\frac{d\zeta_{\gamma-\epsilon,j-1}}{dt} - \frac{d\zeta_{\gamma-\epsilon,j}}{dt} \right) - \frac{E_{\gamma}}{c_{\gamma+\epsilon}} \left(\frac{d\zeta_{\gamma+\epsilon,j-1}}{dt} - \frac{d\zeta_{\gamma+\epsilon,j}}{dt} \right) \quad (5.1)$$

for all levels $j = 2, 3, \dots, J-1$. We note that (5.1) does not apply for the cases $\gamma = 0+i0$. Furthermore, for notational purposes, we will stipulate that in (5.1) and all future relationships, terms which require $\gamma-\epsilon = 0+i0$ or $n_{\gamma-\epsilon} < \zeta_{\gamma-\epsilon}$ do not exist. This applies equally to cases in which $\gamma+\epsilon$ is not contained within the specified model truncation limits.

Let us now define

$$a_{\gamma,j} \equiv -i\ell_{\gamma}(\psi_{\gamma,j-1} - \psi_{\gamma,j}) - A_{\gamma,j-1} + A_{\gamma,j} - \left(\frac{1}{r-1}\right)F_{\gamma,j-1} + \left(\frac{r+1}{r-1}\right)F_{\gamma,j} - \left(\frac{r}{r-1}\right)F_{\gamma,j+1} \quad (5.2)$$

$$b_{\gamma,j} \equiv -B_{\gamma,j} + \left[\frac{R}{C_p 8\Omega^2 a^2}\right]q_{\gamma,j}$$

such that using (4.9) we can write

$$\begin{aligned}
\frac{dc_{Y,j-1}}{dt} - \frac{dc_{Y,j}}{dt} = & a_{Y,j} - \frac{1}{(r-1)} \frac{D_Y}{c_{Y-\epsilon}} [W_{Y-\epsilon,j-1} - (r+1)W_{Y-\epsilon,j} + \\
& + rW_{Y-\epsilon,j+1}] + \frac{1}{(r-1)} \frac{E_Y}{c_{Y+\epsilon}} [W_{Y+\epsilon,j-1} - \\
& - (r+1)W_{Y+\epsilon,j} + rW_{Y+\epsilon,j+1}]
\end{aligned} \tag{5.3}$$

and, the thermodynamic energy equation of (7.11) reduces to

$$\frac{dT_{Y,j}}{dt} = b_{Y,j} - S_j W_{Y,j} \tag{5.4}$$

Inserting solutions (5.3) and (5.4) into (5.1) has the effect of eliminating the time dependence of (5.1) and at any given time we have

$$\begin{aligned}
\Delta Z c_{Y,j} b_{Y,j} - \Delta Z c_{Y,j} S_j W_{Y,j} = & \frac{D_Y}{c_{Y-\epsilon}} a_{Y-\epsilon,j} - \frac{E_Y}{c_{Y+\epsilon}} a_{Y+\epsilon,j} - \\
& - \frac{1}{(r-1)} \frac{D_{Y-\epsilon} D_Y}{c_{Y-2\epsilon} c_{Y-\epsilon}} [W_{Y-2\epsilon,j-1} - (r+1)W_{Y-2\epsilon,j} + rW_{Y-2\epsilon,j+1}] + \\
& + \frac{1}{(r-1)} \left(\frac{E_{Y-\epsilon} D_Y}{c_{Y-\epsilon} c_Y} + \frac{E_Y D_{Y+\epsilon}}{c_Y c_{Y+\epsilon}} \right) [W_{Y,j-1} - (r+1)W_{Y,j} + rW_{Y,j+1}] - \\
& - \frac{1}{(r-1)} \frac{E_Y E_{Y+\epsilon}}{c_{Y+\epsilon} c_{Y+2\epsilon}} [W_{Y+2\epsilon,j-1} - (r+1)W_{Y+2\epsilon,j} + rW_{Y+2\epsilon,j+1}]
\end{aligned}$$

or, if we define

$$\begin{aligned}
z_{Y,j} &\equiv (r-1) \left[\frac{D_Y}{c_{Y-\varepsilon} c_Y} a_{Y-\varepsilon,j} - \frac{E_Y}{c_Y c_{Y+\varepsilon}} a_{Y+\varepsilon,j} - \Delta Z b_{Y,j} \right] \\
f_Y^{(1)} &\equiv \frac{D_{Y-\varepsilon} D_Y}{c_{Y-2\varepsilon} c_{Y-\varepsilon} c_Y} \\
f_Y^{(2)} &\equiv -\frac{1}{c_Y^2} \left(\frac{E_{Y-\varepsilon} D_Y}{c_{Y-\varepsilon}} + \frac{E_Y D_{Y+\varepsilon}}{c_{Y+\varepsilon}} \right) \\
f_Y^{(3)} &\equiv \frac{E_Y E_{Y+\varepsilon}}{c_Y c_{Y+\varepsilon} c_{Y+2\varepsilon}} \\
\sigma_j &\equiv (r-1) \Delta Z S_j
\end{aligned} \tag{5.5}$$

the W-equation can be compacted to

$$\begin{aligned}
& [f_Y^{(1)} W_{Y-2\varepsilon,j-1} + f_Y^{(2)} W_{Y,j-1} + f_Y^{(3)} W_{Y+2\varepsilon,j-1}] - \\
& - (r+1) [f_Y^{(1)} W_{Y-2\varepsilon,j} + f_Y^{(2)} W_{Y,j} + f_Y^{(3)} W_{Y+2\varepsilon,j}] + \\
& + r [f_Y^{(1)} W_{Y-2\varepsilon,j+1} + f_Y^{(2)} W_{Y,j+1} + f_Y^{(3)} W_{Y+2\varepsilon,j+1}] - \\
& - \sigma_j W_{Y,j} = z_{Y,j}
\end{aligned} \tag{5.6}$$

in which from (1.17) we represent the boundary conditions as

$$\begin{aligned}
W_{Y,1} &= 0 \\
W_{Y,J} &= W_{Y,J}(t, \lambda, \mu) \\
&\text{as given from external sources.}
\end{aligned} \tag{5.7}$$

To prepare (5.6) for inversion we want to take note of certain properties of the equations in order to reduce the calculation to a finite set of simple matrix solutions. Inspection of (5.6) shows that the equations uncouple according to planetary wave numbers, ℓ_Y . In addition, within each planetary wave the equations contain two independent sets; one of even vector elements ($n_Y + \ell_Y$ all even) and the others of odd vector elements ($n_Y + \ell_Y$ all odd). Thus, to facilitate ease of notation, let us define some new sets of indices to be applied to (5.6) by first denoting a maximum planetary wave number, L , for a given spectral truncation as

$$L = \ell_Y)_{\max} \quad (5.8)$$

so that we can designate K independent sets of matrix equations using index k where

$$k = 1, 2, 3, \dots, K; K = 2(L+1). \quad (5.9)$$

For a given matrix set we will determine k by designating

$$k = \left\{ \begin{array}{l} 2\ell_Y + 1 \text{ for even vector sets} \\ 2(\ell_Y + 1) \text{ for odd vector sets} \end{array} \right\} \quad (5.10)$$

Furthermore, within each of the K matrix equation sets it is useful to designate an element index, b_k , where

$$b_k = 1, 2, 3, \dots, B_k \quad (5.11)$$

Thus, for a given matrix set designated by the subscript k we devise the b_k indices as follows:

(1) For k odd (even vectors) let

$$N_k = n_k)_{\max} \quad (5.12)$$

for which we consider only n_k from the set $n_k + \ell_k$ even. Then the value for an individual b_k is determined from

$$\left. \begin{aligned} b_k &= \frac{n_k - \ell_k + 2}{2} - \delta_{\ell_k, 0} \\ B_k &= \frac{N_k - \ell_k + 2}{2} - \delta_{\ell_k, 0} \end{aligned} \right\} \quad (5.13)$$

where we ignore values of b_k outside the range indicated in (5.11); i.e., when $k = 1$, $n_1 = 0$, and $\ell_1 = 0$ we do not include the value $b_1 = 0$ which designates the nonallowable equation of (5.1) in which $\gamma = 0+i0$ [see comments following (5.1)].

Similarly,

(2) For k even (odd vectors) let

$$N_k = n_k)_{\max} \quad (5.14)$$

in which here we consider only n_k from the set $n_k + \ell_k$ odd. Then, we have

$$\left. \begin{aligned} b_k &= \frac{n_k - \ell_k + 1}{2} \\ B_k &= \frac{N_k - \ell_k + 1}{2} \end{aligned} \right\} \quad (5.15)$$

At this point we want to note an additional property inherent in the spectral W -equations represented by (5.6). That is, from definitions contained in

(5.5) and Appendix B we can show that for any given k ,

$$f_{b_k}^{(3)} = \frac{E_{Y_k} E_{Y_k^{\dagger \epsilon}}}{c_{Y_k} c_{Y_k^{\dagger \epsilon}} c_{Y_k^{\dagger 2\epsilon}}} \quad (5.16)$$

$$\equiv \frac{D_{Y_k^{\dagger \epsilon}} D_{Y_k^{\dagger 2\epsilon}}}{c_{Y_k} c_{Y_k^{\dagger \epsilon}} c_{Y_k^{\dagger 2\epsilon}}} \equiv f_{b_k^{\dagger 1}}^{(1)}$$

We are now prepared to convert (5.6) to matrix form. To do this we first define tridiagonal matrices D_k as

$$D_k = \begin{pmatrix} f_1^{(2)} & f_1^{(3)} & 0 & \dots & 0 \\ f_1^{(3)} & f_2^{(2)} & f_2^{(3)} & & \\ \vdots & \ddots & \ddots & \ddots & \vdots \\ 0 & f_{b_k-1}^{(3)} & f_{b_k}^{(2)} & f_{b_k}^{(3)} & \\ \vdots & \ddots & \ddots & \ddots & \vdots \\ 0 & \dots & \dots & f_{B_k-1}^{(3)} & f_{B_k}^{(2)} \end{pmatrix}_k \quad (5.17)$$

where we have made use of (5.8) - (5.16). We note from (5.17) that not only is each D_k tridiagonal but it is also symmetric. In addition, it can be shown that every principle minor determinate of D_k is positive and thus D_k can be said to be positive definite. These properties will be discussed in more detail below.

To complete the conversion of (5.6) to matrix form we define vectors

$$W_{k,j} = \begin{pmatrix} w_{1,j} \\ w_{2,j} \\ \vdots \\ w_{B_k,j} \\ \vdots \\ w_{B_k,j} \end{pmatrix}_k ; R_{k,j} = \begin{pmatrix} r_{1,j} \\ r_{2,j} \\ \vdots \\ r_{B_k,j} \\ \vdots \\ r_{B_k,j} \end{pmatrix}_k \quad (5.18)$$

such that (5.6) can be written in the matrix form

$$D_k W_{k,j-1} - (r+1)D_k W_{k,j} + rD_k W_{k,j+1} - \sigma_j W_{k,j} = R_{k,j} ; \quad (5.19)$$

$j = 2, 3, 4, \dots, J-1$ for each $k = 1, 2, 3, \dots, K$

We wish to modify (5.19) through diagonalization of each D_k . However, since each tridiagonal D_k is real, symmetric and positive definite, we know that all eigenvalues of D_k are real and positive. Also, the sets of eigenvectors associated with these eigenvalues are orthonormal. Thus, if D_k is an $M \times M$ matrix, there exists a set of real positive eigenvalues $(\lambda_k)_p$ with $p = 1, 2, 3, \dots, M$ associated with D_k and M sets of orthonormal eigenvectors $q_{p,s}$ with $s = 1, 2, 3, \dots, M$. If we let Q_k represent the matrix of eigenvectors associated with the set $(\lambda_k)_p$ and matrix D_k , we have

$$Q_k = \begin{pmatrix} q_{11} & q_{12} & \cdots & q_{1s} & \cdots & q_{1m} \\ q_{21} & q_{22} & \cdots & q_{2s} & \cdots & q_{2m} \\ \vdots & \vdots & & \vdots & & \vdots \\ q_{p1} & q_{p2} & \cdots & q_{ps} & \cdots & q_{pm} \\ \vdots & \vdots & & \vdots & & \vdots \\ q_{m1} & q_{m2} & \cdots & q_{ms} & \cdots & q_{mm} \end{pmatrix}_k \quad (5.20)$$

such that

$$Q_k \tilde{Q}_k = \tilde{Q}_k Q_k = I \quad (5.21)$$

where I is the unit matrix and $(\tilde{})$ denotes transposition. Define

$$\Lambda_k = \begin{pmatrix} (\lambda_k)_1 & 0 & \dots & \dots & 0 \\ 0 & \ddots & & & \vdots \\ \vdots & & (\lambda_k)_2 & & \vdots \\ \vdots & & & \ddots & \vdots \\ 0 & \dots & \dots & \dots & (\lambda_k)_m \end{pmatrix} \quad (5.22)$$

where then we know

$$\left. \begin{aligned} D_k Q_k &= Q_k \Lambda_k \\ \text{and} \\ \tilde{Q}_k D_k Q_k &= \tilde{Q}_k Q_k \Lambda_k = \Lambda_k \end{aligned} \right\} \quad (5.23)$$

We now want to expand the vector $W_{k,j}$ in (5.19) in the form

$$W_{k,j} = Q_k V_{k,j} ; V_{k,j} = \tilde{Q}_k W_{k,j} \quad (5.24)$$

where we note that $V_{k,j}$ is also a vector.

Inserting solutions (5.24) into (5.19) and multiplying through with \tilde{Q}_k gives

$$\begin{aligned} \tilde{Q}_k D_k Q_k V_{k,j-1} - (r+1) \tilde{Q}_k D_k Q_k V_{k,j} + r \tilde{Q}_k D_k Q_k V_{k,j+1} - \\ - \sigma_j \tilde{Q}_k Q_k V_{k,j} = \tilde{Q}_k R_{k,j} \end{aligned}$$

or, from (5.23), we can write

$$\Lambda_k V_{k,j-1} - [(r+1)\Lambda_k + \sigma_j] V_{k,j} + r v_{k,j+1} = \tilde{Q}_k R_{k,j} \quad (5.25)$$

Now, we know that there exists an inverse

$$\Lambda_k^{-1} = \begin{pmatrix} 1/(\lambda_k)_1 & 0 & \dots & \dots & \dots & 0 \\ 0 & 1/(\lambda_k)_2 & & & & \vdots \\ \vdots & & \ddots & & & \vdots \\ \vdots & & & 1/(\lambda_k)_p & & \vdots \\ \vdots & & & & \ddots & \vdots \\ 0 & \dots & \dots & \dots & \dots & 1/(\lambda_k)_m \end{pmatrix} \quad (5.26)$$

such that

$$\Lambda_k^{-1} \Lambda_k = I. \quad (5.27)$$

Thus, if we multiply (5.25) through with Λ_k^{-1} , (5.25) reduces to the form

$$V_{k,j-1} - [(r+1)I + \sigma_j \Lambda_k^{-1}] V_{k,j} + r v_{k,j+1} = \Lambda_k^{-1} \tilde{Q}_k R_{k,j} \quad (5.28)$$

where for each $k = 1, 2, 3, \dots, K$ we have $j = 2, 3, 4, \dots, j-1$. We now let

$$\begin{aligned} & S_{k,j} \equiv - [(r+1)I + \sigma_j \Lambda_k^{-1}] \\ \text{and} & R_{k,j} \equiv \left\{ \begin{array}{l} \Lambda_k^{-1} \tilde{Q}_k R_{k,2} - v_{k,1} \quad (\text{for } j = 2) \\ \Lambda_k^{-1} \tilde{Q}_k R_{k,j} \quad (\text{for } 3 \leq j \leq j-2) \\ \Lambda_k^{-1} \tilde{Q}_k R_{k,j-1} - r v_{k,j} \quad (\text{for } j = j-1) \end{array} \right\} \quad (5.29) \end{aligned}$$

Using (5.29), (5.28) transforms to the set

$$\left. \begin{aligned}
 S_{k,2}V_{k,2} + r V_{k,3} &= R_{k,2} & (\text{for } j = 2) \\
 V_{k,j-1} + S_{k,j}V_{k,j} + r V_{k,j+1} &= R_{k,j} & (3 \leq j \leq J-2) \\
 V_{k,J-2} + S_{k,J-1}V_{k,J-1} &= R_{k,J-1} & (\text{for } j = J-1)
 \end{aligned} \right\} \quad (5.30)$$

in which from (5.24) and the boundary conditions of (5.7) we see that in (5.29)

$$\left. \begin{aligned}
 V_{k,1} &= 0 \\
 V_{k,J} &= \tilde{Q}_k W_{k,J}
 \end{aligned} \right\} \quad (5.31)$$

We see that for each k the system (5.30) is tridiagonal in j and thus submits readily to solution provided certain provisions are met (see Appendix C for details). Briefly, to invert (5.30) we first define

$$\left. \begin{aligned}
 u_{k,2} &\equiv S_{k,2}^{-1} & (\text{for } j = 2) \\
 u_{k,j} &\equiv (S_{k,j} - r u_{k,j-1})^{-1} & (\text{for } 3 \leq j \leq J-1) \\
 v_{k,j} &\equiv -r u_{k,j} & (2 \leq j \leq J-1)
 \end{aligned} \right\} \quad (5.32)$$

and then let

$$\left. \begin{aligned}
 y_{k,2} &= u_{k,2} R_{k,2} & (\text{for } j = 2) \\
 y_{k,j} &= u_{k,j} (R_{k,j} - y_{k,j-1}) & (\text{for } 3 \leq j \leq J-1)
 \end{aligned} \right\} \quad (5.33)$$

Solutions to (5.30) thus appear as

$$\begin{aligned}
 v_{k,J-1} &= y_{k,J-1} && \text{(for } j = J-1) \\
 v_{k,j} &= v_{k,j} v_{k,j+1} + y_{k,j} && \text{(for } j = J-2, J-3, \dots, 2)
 \end{aligned}
 \left. \vphantom{\begin{aligned} v_{k,J-1} \\ v_{k,j} \end{aligned}} \right\} \quad (5.34)$$

provided all $u_{k,j}$ in (5.23) exist and are finite. Vectors $w_{k,j}$ are then obtained from (5.24).

6. The model codes

The model consists of four separate programs, three of which are preliminary and need to be executed only once. The names of the four programs are ITCOF1, ITCOF2, MESOS1, and MESOS2. A brief description of each of these follows.

ITCOF1, ITCOF2

ITCOF1 and ITCOF2 are used consecutively to generate and store on the system disk a set of non-linear interaction coefficients for use in computing the non-linear Jacobians in the model. The definition and method used for the computation of the interaction coefficients are contained in Appendix A.

To run ITCOF1, use file RUNIC1 (see Figure 6.1). This routine requires disk files INTCOEF1 and STRAT1 as input and creates a file named IC1OUT as output. IC1OUT is used as input by ITCOF2.

The program RUNIC2 (Figure 6.2) drives ITCOF2 and requires files INTCOEF2, STRAT1, and IC1OUT as input. ITCOF2 creates a file IC2OUT on output which contains the interaction coefficient and instruction fields required by the model.

MESOS1

MESOS1 is an initializing program which creates and stores all constants, truncation parameters, transform parameters, and fixed fields required for the particular model configuration to be run. This program must be run prior to the beginning of a particular model experiment and, in general, calculates everything that can be done for the model in advance outside of the main iterative loop.

MESOS1 is driven by the file MESOSBEG (Figure 6.3) and requires input files STRAT1 and IC2OUT. On output, the file MESOS1Ø will contain all of the input

fields required by the model except for the model's initial conditions. In addition, a set of data which includes horizontal mean temperatures and stabilities is required as input as shown in Figure 6.3.

MESOS2

MESOS2 represents the central loop of the model. It is called into action by the file MESOSSTART (Figure 6.4) which requires input files STRAT2, MESOS10, INITDEC, BNDFILE, and HEATFILE. The last three of these are data files which include the initial conditions file, the lower boundary conditions file, and the temporary heating file respectively. MESOS10 is as described above under MESOS1.

On output, the file MESOUT11 contains the complete history of the model run. The model can be restarted as often as required from this history file and the subsequent output is appended onto the file. The first records on MESOUT11 contain fixed model parameters. Subsequent records are each made up of a time step number, the spectral vorticity coefficients, the spectral vertical velocity coefficients and, if applicable, the spectral ozone mixing ratio coefficients for the particular time step.

An additional file is provided in the program to include the spectral coefficient values for all the non-linear terms in the model at each time step. This is assigned to "TAPE13" but is currently not being retained by the model as a permanent file.

The first pages of the listings for the model programs ITCOF1, ITCOF2, MESOS1, and MESOS2 are shown in Figures 6.5 - 6.8 for purposes of reference.

```

*** PROGRAM RUNIC1 ***
RICF1,TS9,CM120000.
ATTACH(OLDPL,INTCOEF1,ID=ALYEA)
UPDATE(IF,P=OLDPL)
RETURN(OLDPL)
FTN(L=0,I=COMPILE)
ATTACH(OLDPL,STRAT1,ID=ALYEA)
UPDATE(IF,P=OLDPL,Q)
FTN(L=0,I=COMPILE,B=LOG)
REQUEST(TAPE9,MPF)
LOAD(LGO,LOG)
EXECUTE.
CATALOG(TAPE9,IC1OUT,ID=ALYEA,RP=999)
M/NEOR CDC END-OF-RECORD
M/NEOR CDC END-OF-RECORD
HIDENT COMPAC
HDELETE COMPACK.5
USE /PKBLK/
R_COMPILE COMPACK
M/NEOR CDC END-OF-RECORD
J(A,B) -- EVEN + ODD
2 6 6 3
M/NEOF CDC END-OF-FILE

```

Figure 6.1: Program RUNIC1.

```

*** PROGRAM RUNIC2 ***
RICF2,T59,CM120000.
ATTACH(OLDPL,INTCOEF2, ID=ALYEA)
UPDATE(IF,P=OLDPL)
RETURN(OLDPL)
FTN(L=0, I=COMPILE)
ATTACH(OLDPL,STRAT1, ID=ALYEA)
UPDATE(IF,P=OLDPL,Q)
FTN(L=0, I=COMPILE, B=LOG)
ATTACH(TAPE9, IC1OUT, ID=ALYEA)
LOAD(LOG, LOG)
EXECUTE.
CATALOG(TAPE10, IC2OUT, ID=ALYEA, RP=999)
#NEOR CDC END-OF-RECORD
#NEOR CDC END-OF-RECORD
#IDENT COMPAK
#DELETE COMPACK.5
USE /PKBLK/
#COMPILE COMPACK
#NEOR CDC END-OF-RECORD
#NEOR CDC END-OF-FILE

```

Figure 6.2: Program RUNIC2.

```

*** PROGRAM MESOSBEG ***
INIT1,T59,CM267100.
ATTACH(OLDPL,STRAT1, ID=ALYEA)
ATTACH(TAPE10,IC2OUT, ID=ALYEA)
UPDATE(IF,P=OLDPL)
RETURN(OLDPL)
FTN(L=O,T,I=COMPILE)
RETURN(COMPILE)
REQUEST(TAPE12,MPF)
LDSET(PRESET=ZERO)
LGO.
CATALOG(TAPE12,MESOS10, ID=ALYEA, RP=999)
#/#OR CDC END-OF-RECORD
#IDENT APR
#DELETE STRAT1.2
PROGRAM MESOS1 (INPUT,OUTPUT,TAPE5=INPUT,TAPE6=OUTPUT,TAPE10,
#DELETE STRAT1.4
#DELETE STRAT1.10
#DELETE STRAT1.32
C CALL VDIST(XIBAR,1,INVERT,0)
#DELETE STRAT1.33
C CALL HDIST(H,1,INVERT,2)
#DELETE STRAT1.34
C CALL ZONTS
#DELETE STRAT1.35
C CALL EDDYTS
#DELETE STRAT1.36
C CALL OVLAP
#DELETE STRAT1.39
C CALL DIFFK(1,DIFFM)
#DELETE STRAT1.40
C CALL DIFFK(2,DIFFX)
#DELETE STRAT1.49
C CALL XOSEQU
#DELETE ZLEV.6
DATA NV26,R26,Z0/26,2.12472,6.08205/
#INSERT ZLEV.8
ZTOP=ZTOP+Z0
#DELETE ZLEV.28
WRITE(6,900) DZ,RVERT,Z0
#DELETE ZLEV.29
900 FORMAT(IH0,14X,#DZ = #,F10.6,# RVERT = #,F10.6,
1 # Z0 = #,F10.6)
#DELETE INITIAL.1,APROXJ.33
#/#OR CDC END-OF-RECORD
5 6 26 1
1 26
962.5 995.5 HORIZONTAL MEAN TEMPERATURE DATA
702.0 930.5 991.0
257.0 583.5 878.5
187.0 212.5 459.5
208.5 187.0 197.0
267.0 219.5 191.0
981.0 231.0 200.0
245.0 254.5 347.0

```

Figure 6.3: Program MESOSBEG.

*** PROGRAM MESOSBEG ***

1	26	289.01
308.45		321.53
345.16		327.56
162.65		100.51
55.41		50.76
46.62		47.77
59.96		80.58

HORIZONTAL MEAN STABILITY DATA

292.70
336.53
288.16
71.20
45.93
49.07
88.62

299.13
346.05
233.47
60.91
45.52
50.08

NLON, NLAT= 16 15
E/NEOF CDC END-OF-FILE

Figure 6.3 continued.

```

*** PROGRAM MESOSSTART ***
START, T50, CM210100, EC155.
ATTACH(OLDPL, STRAT2, ID=ALYEA)
UPDATE (F)
RETURN(OLDPL)
FTN(L=0, T, I=COMPILE)
RETURN(COMPILE)
ATTACH(TAPE10, MESOS10, ID=ALYEA)
ATTACH(TAPE12, INITDEC, ID=ALYEA)
ATTACH(TAPE14, BNDFILE, ID=ALYEA)
ATTACH(TAPE15, HEATFILE, ID=ALYEA)
REQUEST(TAPE11, #PF)
REQUEST(TAPE13, #PF)
LGO.
CATALOG(TAPE11, MESOUT11, ID=ALYEA, RP=999)
AUDIT, ID=ALYEA.
#/#EOR CDC END-OF-RECORD
#/#EOR CDC END-OF-RECORD
0 4
4 1.0 -110
RUN 34 AMES TEST RUN WITH NOX, OH. STARTS DEC. 1
1 0
#/#EOF CDC END-OF-FILE

```

Figure 6.4: Program MESOSSTART.

```

*DECK ICOF1
PROGRAM ITCOF1(INPUT,OUTPUT,TAPES=INPUT,TAPE6=OUTPUT,TAPE9)
DOUBLE PRECISION ZER0,Z1,COEF,WORK,AR,W,D,ARG,DLAT,P,PLN,
1 AP,BP,PPLN
C
COMMON ZER0(50),ZER01(50),Z1(50),COEF(50),AR(50),W(50),D(30),
1 ARG(50),DLAT(50),P(50),PLN(169,19),AP(156,19),BP(156,19),KMAX,
2 KP1,IERR,LP1,IH
C
DIMENSION PPLN(13,13,19),WORK(50),JCOEF(110)
C
READ(5,890) JCOEF
FORMAT(10A4)
890 READ(5,900) IH,LR,NZON,ITERM
900 FORMAT(16I5)
C
FOR ITERM DEFINITION SEE NOTE AT THE BEGINNING
C
JUMP=MOD(IH,2)
NR=NZON
LP1=NR+1
GO TO (3,4,5,6,7,8),ITERM
C
3 KMAX=NZON+LR+1
GO TO 10
4 KMAX=LR+1.5*NZON+.5000000001
GO TO 10
5 KMAX=LR+1.5*NZON+.5000000001
GO TO 10
6 KMAX=NZON+1
GO TO 10
7 KMAX=1.5*NZON+1.0001
GO TO 10
8 KMAX=1.5*NZON+.50001
C
10 CONTINUE
CALL GAUSWT(ICOUNT,WORK)
WRITE(6,997) ICOUNT
997 FORMAT(IH,10X,NSUB,GAUSWT,ICOUNT=*,I3)
IF(IERR.GT.0) GO TO 2
KMAX=ICOUNT
C
COMPUTATION OF LEGENDRE POLYNOMIAL VALUES
C
ICOUNT=0
IJP=2
IF(IH.EQ.2) IJP=1
DO 30 L=1,LP1
LL=L-1
NP1=LL+NZON+2
DO 30 NH=L,NP1,IJP
N=NH-1+JUMP
ICOUNT=ICOUNT+1
34 CALL KUGELU(LL,M,KMAX,AR,P,WORK)

```

Figure 6.5: First page of Program ITCOF1.

```

*DECK ICOF2
PROGRAM ITCOF2(INPUT,OUTPUT,TAPE5=INPUT,TAPE6=OUTPUT,TAPE9,
1 TAPE10)
DOUBLE PRECISION COEF,W,P,AP,BP,C
COMMON W(50),P(156,19),AP(156,19),BP(156,19),C(180),KMAX
COMMON /PKBLK/ NS,N1,N2,N3,N4,LS,L1,L2,L3,L4
DIMENSION INST(40,20),COEF(2000),IS(1000),KD(180,6),MTYPE(10)

C
ICK=0
DO 5 I=1,40
DO 5 J=1,20
5 INST(I,J)=0

C
READ(I) MTYPE
WRITE(6,9001) MTYPE
READ(I) JH,LR,NR,ITERM,ICOUNT,KMAX,LR1,NR1,IJP,(W(I),I=1,KMAX),
1 ((P(I,J),J=1,KMAX),I=1,ICOUNT),((AP(I,J),J=1,KMAX),I=1,ICOUNT),
2 ((BP(I,J),J=1,KMAX),I=1,ICOUNT)

C
READ(5,1) LBEG,LSTP,ISKIP
WRITE(6,1230) LR,NR,LBEG,LSTP,ISKIP
IF(LBEG.EQ.0) WRITE(10) MTYPE,LR,NR
LBEG=LBEG+1
LSTP=LSTP+1
L=LR+1
M=NR+1
I=0
DO 10 L2=1,L
LL=L2
NN=LL+N-1
DO 10 L1=LL,NN
I=I+1
10 INST(L1,L2)=I
WRITE(6,9000)
WRITE(6,9001) LR,NR
WRITE(6,9002)
NN=LL+N-1
DO 20 I=1,NN
I2=NN-I+1
I21=I2-1
20 CONTINUE
WRITE(6,9003) I21,(INST(I2,J),J=1,L)
DO 25 I=1,L
IS(I)=I-1
25 WRITE(6,9004) (IS(I),I=1,L)
LL=2*LL-1
ITOT=0
ISTOT=0
DO 800 LGI=LBEG,LSTP
INDEX=0
INS=0
LGI=LGI-1
DO 700 LBI=1,LL

```

Figure 6.6: First page of Program ITCOF2.


```

STRAT1 1 A
STRAT1 1 A
STRAT1 3 A
STRAT1 5 A
STRAT1 6 A
STRAT1 7 A
STRAT1 8 A
STRAT1 9 A
STRAT1 11 A
STRAT1 12 A
STRAT1 13 A
STRAT1 14 A
STRAT1 15 A
STRAT1 16 A
STRAT1 17 A
STRAT1 18 A
STRAT1 19 A
STRAT1 20 A
STRAT1 21 A
STRAT1 22 A
STRAT1 23 A
STRAT1 24 A
STRAT1 25 A
STRAT1 26 A
STRAT1 27 A
STRAT1 28 A
STRAT1 29 A
STRAT1 30 A
STRAT1 31 A
APR 2 A
APR 3 A
APR 4 A
APR 5 A
APR 6 A
STRAT1 37 A
STRAT1 38 A
APR 7 A
APR 8 A
STRAT1 41 A
STRAT1 42 A
STRAT1 43 A
STRAT1 44 A
STRAT1 45 A
STRAT1 46 A
STRAT1 47 A
STRAT1 48 A
APR 9 A
STRAT1 50 A
STRAT1 51 A
STRAT1 52 A
STRAT1 53 A
STRAT1 54 A

PROGRAM MESOS1 INPUT, OUTPUT, TAPES=INPUT, TAPE6=OUTPUT, TAPE10,
1 TAPE12)
DOUBLE PRECISION A
COMMON A(700), IM(300), CTYPE(10), XDMP1(8500)
COMMON /COFBLK/ C(3800), IS(1500)
COMMON /CONSTS/ INDEX, NR, LR, INS, INSZ, KINT, ILEV1, ILEV2, NVERT,
1 NRTP, LRTP, NTYP, NVECT, NVREAL, NVZON, NCYC, DT
COMMON /PKBLK/ NS, N1, N2, N3, N4, LS, L1, L2, L3, L4
COMMON /CGBLK/ KD(43), CG(43), NCOMP(12), LWAVE(12), NV(43), LV(43)
COMMON /DEBLK/ DG(43), EG(43), DCG(43)
COMMON /EIGBLK/ ERECT(126), XLIVET(126), EVAL(42), NRK(14), K
COMMON /VHTBLK/ ZVAL(26), PVAL(26), VWT(26), DZ, RVERT
COMMON /BARBLK/ TBAR(26), SIGMA(26), XIBAR(26), DIFFM(26), DIFFX(26)
1, DIFFMB(26), DIFFXB(26), JBM1, JBM2, JBX1, JBX2
COMMON /FTCST/ NLOW, NLAT, NGRID, ARSP(30), XDMP2(30)
COMMON /HEATBK/ H(26), TZSON(104), TSEDDY(16), I1TSZ, I2TSZ, I1TSW,
1 I2TSW, MERGE1, MERGE2, ZWT1(5), ZWT2(5), Q3WR(5)
COMMON /UVBLK/ U(1092), V(1092)
COMMON /FFT/ WP(7,7,15), NW(2,7), NTRANS(16), NNN, NM, LR1, NLATF,
1 NCPAR(7), LOGN
COMMON /GLOP/ PML(7,7,15), WT(50), AR(50)
DIMENSION FX(26), X(26), B(26)
CALL TRUNC
CALL DGEQ
CALL EIGSOL
CALL ZLEV
CALL VDIST (TBAR, 1, NVERT, 1)
CALL VDIST (SIGMA, 1, NVERT, 1)
CALL VDIST (XIBAR, 1, NVERT, 0)
CALL HDIST (H, 1, NVERT, 2)
CALL ZONTS
CALL EDDYTS
CALL OVLAP
STRAT1 ILEV1=1
STRAT1 ILEV2=NVERT-1
STRAT1 CALL DIFFK(1, DIFFM)
STRAT1 CALL DIFFK(2, DIFFX)
STRAT1 ILEV1=2
STRAT1 ILEV2=NVERT-1
STRAT1 ILEV2=NVERT-1
STRAT1 CALL UVMAT
STRAT1 READ (5, 1000) NLOW, NLAT
STRAT1 FORMAT (10X, 14I5)
STRAT1 NGRID=NLON*NLAT
STRAT1 CALL FFTINT
STRAT1 CALL XOSEQU
STRAT1 WRITE (6, 1010) NLOW, NLAT, NGRID
STRAT1 FORMAT (10I0, 10X, #NLON = #, 13, #, NLAT = #, 13, #, NGRID = #, 16, #, #)
STRAT1 1010 CALL WRT12
STRAT1 STOP
STRAT1 END

```

Figure 6.7: First page of Program MESOS1

```

*DECK STRAT2
STRAT2 PROGRAM MESOS2(INPUT,OUTPUT,TAPE5=INPUT,TAPE6=OUTPUT,TAPE9,
STRAT2 1 TAPE10,TAPE11,TAPE12,TAPE13,TAPE14,TAPE15)
STRAT2
STRAT2 PROGRAM MESOS2
STRAT2 LEVEL 3,C,HTSVE,IS,OSV,TOPO,TPMGRD,DUM2,CHDUM,X03SV,DX03DT
STRAT2 COMMON PSI(2060),ZETA(2060),Z1(2060),T(2060),Z2(2060),X0X(2060),
STRAT2 1 Z3(2060)
STRAT2 COMMON /COFBLK/ C(3900), IS(1500)
STRAT2 COMMON /CONSTS/ INDEX,MR,LR,INS,IMSZ,KINT,ILEV1,ILEV2,NVERT,NRTP,
STRAT2 1 LRTP,NTPY,NVECT,NVREAL,NVZON,NCYC,DT,YRLAG,TIME
STRAT2 COMMON /CGBLK/ KD(43),CG(43),NGOMP(12),LWAVE(12),NV(43),LV(43)
STRAT2 COMMON /DEBLK/ DG(43),EG(43),DECG(43),EGCG(43)
STRAT2 COMMON /EIGBLK/ EVEC(126),XLIVET(126),EVAL(42),NRK(14),KNR
STRAT2 COMMON /VRTBLK/ ZVAL(26),PVAL(26),VWT(26),DZ,RV
STRAT2 COMMON /DERIV/ VDERIV(2366),TDERIV(2366),W(2366)
STRAT2 COMMON /BARBLK/ TBAR(26),SIGMA(26),XBAR(26),DIFFM(26),DIFFX(26)
STRAT2 COMMON /HEATBK/ H(26),TSZON(104),TSEDDY(16),ITTSZ,ITTSZ,ITTSW,
STRAT2 1 I2TSW,MERGE1,MERGE2,ZWT(15),ZWT2(15),Q3WR(15)
STRAT2 COMMON /OROGRA/ TOPO(91),QSV(105),HTSVE(2060)
STRAT2 COMMON /WORKBK/ WORK(7920),OPO(91),SHIRK(10709)
STRAT2 COMMON /QJBLK/NZJ,L103,COLOS(26),LEVPCH,LEVDYN
STRAT2 COMMON /TEMPBK/ ADVSV(182)
STRAT2 COMMON /CHEM/ TMPGRD(5280)
STRAT2 COMMON /SPECIE/ DUM2(19866)
STRAT2 COMMON /FTCST/ NLON,NLAT,NGRID,MORE(30),XDMP2(50)
STRAT2 COMMON /O3OX/ CHDUM(5590)
STRAT2 COMMON /PREDIC/A,B,N,TIMSV(135)
STRAT2 COMMON /GENER/ DX03DT(2366)
STRAT2
STRAT2 COMMON /BND/TBOUND(79),WBOUND(79),X0XBND(79)
STRAT2 COMMON /SHEAT/SQ(474)
STRAT2
STRAT2 DIMENSION X03SV(790)
STRAT2 EQUIVALENCE (CHDUM(2401),X03SV(1))
STRAT2 DIMENSION SPACE(2400),DATAIM(6240),X3SPC(790)
STRAT2 EQUIVALENCE (WORK(1),SPACE(1)),(DATAIM(1),SHIRK(1))
STRAT2 EQUIVALENCE (WORK(2401),X3SPC(1))
STRAT2 DATA NWRT /2/
STRAT2 L103=2
STRAT2 DO 10 I=1,2060
STRAT2 PSI(I)=0.0
STRAT2 ZETA(I)=0.0
STRAT2 T(I)=0.0
STRAT2 Z1(I)=0.0
STRAT2 Z2(I)=0.0
STRAT2 Z3(I)=0.0
STRAT2 W(I)=0.0
STRAT2
STRAT2 10 CONTINUE
STRAT2 CALL READ3
STRAT2 CALL READ10
STRAT2 CALL NLNADJ
STRAT2
STRAT2

```

Figure 6.8: First page of Program MESOS2.

References

- Adams, G. W., 1974: Sources and Sinks of Energy in the Lower Thermosphere. NOAA Technical Report ERL 304-SEL 28, 231 pp.
- Ching, B.K., and Y.T. Chiu, 1973: A phenomenological model of global ionospheric electron density in the E-, F1- and F2-regions. J. Atmos. Terr. Phys., 35, 1615-1630.
- Cunnold, D., F. Alyea, N. Phillips and R. Prinn, 1975: A three-dimensional dynamical-chemical model of atmospheric ozone. J. Atmos. Sci., 32, 170-194.
- Hudson, R.D., and S.H. Mahle, 1972: Photodissociation rates of molecular oxygen in the mesosphere and lower thermosphere. J. Geophys. Res., 77(16), 2902-2914.
- Lindzen, R., and R. Goody, 1965: Radiative and photo-chemical processes in mesospheric dynamics: Part I. Models for radiative and photochemical processes. J. Atmos. Sci., 4, 341-348.
- Lorenz, E., 1960: Energy and numerical weather prediction. Tellus, 12, 364-373.
- Lorenz, E., 1971: An N-cycle time-differencing scheme for stepwise numerical integration. Mon. Wes. Rev., 99, 644-648.
- National Oceanic and Atmospheric Administration, National Aeronautics and Space Administration, and United States Air Force, 1976: U. S. Standard Atmosphere, 1976, U.S. Govt. Printing Office, Washington, D.C., No. 003-017-00323-0.
- Stolarski, R.S., P.B. Hays, and R.G. Roble, 1975: Atmospheric heating by solar EUV radiation. J. Geophys. Res., 80(16), 2266-2276.

Appendix A. Spectral form of Jacobian terms and evaluation of the associated nonlinear interaction coefficients.

Consider on the unit sphere the Jacobian of arbitrary horizontal global scalars A and B where

$$J(A,B) = \frac{\partial A}{\partial \lambda} \frac{\partial B}{\partial \mu} - \frac{\partial A}{\partial \mu} \frac{\partial B}{\partial \lambda} \quad (A.1)$$

and λ is longitude while μ is the sine of latitude. Expanding A and B in terms of spherical harmonics, we have for solutions

$$\left. \begin{aligned} A &= \sum_{\alpha} a_{\alpha} Y_{\alpha}(\lambda, \mu), \\ B &= \sum_{\alpha} b_{\alpha} Y_{\alpha}(\lambda, \mu), \\ \alpha &= n_{\alpha} + i\ell_{\alpha} \end{aligned} \right\} \quad (A.2)$$

in which the special properties of the orthonormal spherical functions $Y_{\alpha}(\lambda, \mu)$ are outlined in (4.3) - (4.8). Inserting solutions (A.2) into (A.1), transforming the result to insure symmetry with respect to vector indices α and β , and writing in terms of a single nonredundant sum (for details of these developments, see Baer and Platzman, 1961) we arrive at

$$J(A,B) = -i \sum_{\substack{\alpha, \beta \\ n_{\beta} > n_{\alpha}}} \left[1 - \frac{E_{\alpha, \beta}}{2} \right] (a_{\alpha} b_{\beta} - a_{\beta} b_{\alpha}) e^{i(\ell_{\alpha} + \ell_{\beta})\lambda} \left(\ell_{\beta} P_{\beta d\mu}^{\alpha} - \ell_{\alpha} P_{\alpha d\mu}^{\beta} \right) \quad (A.3)$$

for which we define through use of the Kronecker delta, $\delta_{i,j}$,

$$E_{\alpha, \beta} \equiv \delta_{n_{\alpha}, n_{\beta}} \delta_{|\ell_{\alpha}|, |\ell_{\beta}|} \quad (A.4)$$

The term $\left[1 - \frac{E_{\alpha, \beta}}{2} \right]$ is necessary because the two conjugate interactions for the

case $n_\beta = n_\alpha$ and $|\ell_\beta| = |\ell_\alpha|$, assumed in the symmetric reduction of $J(A,B)$ to the form of (A.3), are not unique and one of them must be ignored.

We now multiply (A.3) with any arbitrary member of the orthogonalizing set, say $Y_Y^*/4\pi$, and integrate over the unit sphere to get

$$\begin{aligned}
 C_Y &= \frac{1}{4\pi} \int_0^{2\pi} \int_{-1}^1 J(A,B) Y_Y^*(\lambda, \mu) d\mu d\lambda \\
 &= -i \sum_{\alpha, \beta} \left(1 - \frac{E_{\alpha, \beta}}{2} \right) (a_\alpha b_\beta - a_\beta b_\alpha) K_{Y, \beta, \alpha} \\
 &\quad \left\{ \begin{array}{l} n_\beta \geq n_\alpha \\ \ell_Y = \ell_\alpha + \ell_\beta \end{array} \right\}
 \end{aligned} \tag{A.5}$$

and the interaction coefficient, $K_{Y, \beta, \alpha}$ is obtained from

$$K_{Y, \beta, \alpha} \equiv \frac{1}{2} \int_{-1}^1 \left(\ell_\beta P_\beta \frac{dP_\alpha}{d\mu} - \ell_\alpha P_\alpha \frac{dP_\beta}{d\mu} \right) P_Y d\mu. \tag{A.6}$$

Since we intend to evaluate $K_{Y, \beta, \alpha}$ using the "transform" method with integration by exact Gaussian quadrature (see, for example, Eliassen et al., 1970), a time saving simplification can be obtained by noting that the integral in (A.6) can be nonzero only if the integrand possesses an even parity with respect to the equator. For this condition we can reduce (A.6) to

$$K_{Y, \beta, \alpha} = \int_0^1 \left(\ell_\beta P_\beta \frac{dP_\alpha}{d\mu} - \ell_\alpha P_\alpha \frac{dP_\beta}{d\mu} \right) P_Y d\mu. \tag{A.7}$$

In order to evaluate (A.7) numerically let us define

$$\left. \begin{aligned} f_{\alpha}(\mu) &\equiv \ell_{\alpha} P_{\alpha}(\mu) \\ g_{\alpha}(\mu) &\equiv \frac{dP_{\alpha}(\mu)}{d\mu} \end{aligned} \right\} \quad (\text{A.8})$$

where g_{α} can be determined from the Legendre differential relationships in the form

$$\left. \begin{aligned} g_{\alpha}(\mu) &\equiv \frac{dP_{\alpha}(\mu)}{d\mu} \\ &= \frac{(n_{\alpha}+1)\mu P_{\alpha}}{(1-\mu^2)} - \frac{(2n_{\alpha}+1)}{(1-\mu^2)} \left[\frac{(n_{\alpha}+\ell_{\alpha}+1)(n_{\alpha}-\ell_{\alpha}+1)}{(2n_{\alpha}+1)(2n_{\alpha}+3)} \right]^{1/2} P_{\alpha+\ell_{\alpha}}, \\ \epsilon &\equiv 1 + i0 \end{aligned} \right\} \quad (\text{A.9})$$

We now let

$$\begin{aligned} H_{\beta,\alpha}(\mu) &= \ell_{\beta} P_{\beta} \frac{dP_{\alpha}}{d\mu} - \ell_{\alpha} P_{\alpha} \frac{dP_{\beta}}{d\mu} \\ &= f_{\beta} g_{\alpha} - f_{\alpha} g_{\beta} \end{aligned} \quad (\text{A.10})$$

which can be expanded in the form

$$H_{\beta,\alpha}(\mu) = \sum_{\delta} h_{\delta,\beta,\alpha} P_{\delta}(\mu) \quad (\text{A.11})$$

From (A.10) and (A.11) we see that (A.7) can be replaced with

$$\left. \begin{aligned} K_{\gamma,\beta,\alpha} &= \int_0^1 [H_{\beta,\alpha}(\mu)] P_{\gamma} d\mu \\ &= \sum_{\delta} h_{\delta,\beta,\alpha} \int_0^1 P_{\delta} P_{\gamma} d\mu \\ &= h_{\gamma,\beta,\alpha} \end{aligned} \right\} \quad (\text{A.12})$$

However, if we represent $H_{\beta,\alpha}(\mu)$ at N discrete points μ_k where $k = 1, 2, \dots, N$, then an exact quadrature analog for (A.12) is obtained in the form (see Eliassen et al., 1970)

$$\begin{aligned} K_{\gamma,\beta,\alpha} &= \sum_{k=1}^N W_k [H_{\beta,\alpha}(\mu_k)] P_{\gamma}(\mu_k) \\ &= \sum_{k=1}^N W_k [f_{\beta}(\mu_k) g_{\alpha}(\mu_k) - f_{\alpha}(\mu_k) g_{\beta}(\mu_k)] P_{\gamma}(\mu_k) \end{aligned} \quad (\text{A.13})$$

provided

$$\left. \begin{aligned} N &= (\kappa + 1)/2 \\ \kappa &\geq \ell_{\max} + \frac{3}{2} (n_{\max} - \ell_{\max}) + \frac{1}{2} \end{aligned} \right\} \quad (\text{A.14})$$

(N and κ must be intergers) and the latitudes μ_k are located at the Northern Hemisphere zeroes of the Legendre polynomial $P_{\kappa}^0(\mu)$ (including the equator if κ is odd). In (A.13) the W_k represent the Gaussian weights required to maintain orthogonalization of the discrete set of Legendre polynomials used in (A.13) such that

$$\sum_{k=1}^N W_k P_{\alpha}(\mu_k) P_{\beta}(\mu_k) = \delta_{\alpha,\beta} \quad (\text{A.15})$$

A discussion of the evaluation of these Gaussian weights is contained in Appendix D.

References

Baer, R., and G. W. Platzman, 1961: A procedure for numerical integration of the spectral vorticity equation. J. Meteor., 18, 393-401.

Eliassen, E., B. Mackenhauer and E. Rasmussen, 1970: On a numerical method for integration of the hydrodynamical equations with a spectral representation of the horizontal fields. Report No. 2, Institut for Teoretisk Meteorologi, Kobenhavns Universitet, 37 pp.

Appendix B. Spectral representation of divergence terms of the general form

$\nabla \cdot \mu \nabla A.$

In terms of spherical operators on the unit sphere in which λ is longitude and μ is the sine of latitude we have

$$\begin{aligned} \nabla \cdot \mu \nabla A &= \nabla \mu \cdot \nabla A + \mu \nabla^2 A \\ &= (1-\mu^2) \frac{\partial A}{\partial \mu} + \mu \nabla^2 A \end{aligned} \tag{B.1}$$

in which A is an arbitrary horizontal global scalar expandable in the form

$$A = \sum_{\alpha} a_{\alpha} Y_{\alpha}(\lambda, \mu) \tag{B.2}$$

Properties of the orthonormal spherical functions $Y_{\alpha}(\lambda, \mu)$ are outlined in (4.3) - (4.8). Insertion of solutions (B.2) into (B.1) yields

$$\begin{aligned} \nabla \cdot \mu \nabla A &= (1-\mu^2) \sum_{\alpha} a_{\alpha} e^{i\ell_{\alpha}\lambda} \frac{dP_{\alpha}(\mu)}{d\mu} - \mu \sum_{\alpha} c_{\alpha} a_{\alpha} e^{i\ell_{\alpha}\lambda} P_{\alpha}(\mu) \\ &= \sum_{\alpha} a_{\alpha} e^{i\ell_{\alpha}\lambda} \left[(1-\mu^2) \frac{dP_{\alpha}}{d\mu} - \mu c_{\alpha} P_{\alpha} \right], \\ c_{\alpha} &= n_{\alpha}(n_{\alpha}+1) \end{aligned} \tag{B.3}$$

But, if we define

$$\begin{aligned} N_{\alpha} &= \left[\frac{(2n_{\alpha}+1)(n_{\alpha}-\ell_{\alpha})!}{(n_{\alpha}+\ell_{\alpha})!} \right]^{1/2} \\ \epsilon &= 1 + i0 \end{aligned} \tag{B.4}$$

then we know from the Legendre differential and recurrence relations (for example, see Jahnke and Emde, 1945) that

$$(1-\mu^2)\frac{dP}{d\mu} = -n_{\alpha}\mu P_{\alpha} + (n_{\alpha}+\ell_{\alpha})\frac{N_{\alpha}}{N_{\alpha-\epsilon}} P_{\alpha-\epsilon}$$

and

$$\mu P_{\alpha} = \frac{(n_{\alpha}-\ell_{\alpha}+1)}{(2n_{\alpha}+1)} \frac{N_{\alpha}}{N_{\alpha+\epsilon}} P_{\alpha+\epsilon} + \frac{(n_{\alpha}+\ell_{\alpha})}{(2n_{\alpha}+1)} \frac{N_{\alpha}}{N_{\alpha-\epsilon}} P_{\alpha-\epsilon}$$

(B.5)

Then, using (B.5), we can show that

$$(1-\mu^2)\frac{dP}{d\mu} - \mu C_{\alpha} P_{\alpha} = \frac{(1-n_{\alpha}^2)(n_{\alpha}+\ell_{\alpha})}{(2n_{\alpha}+1)} \frac{N_{\alpha}}{N_{\alpha-\epsilon}} P_{\alpha-\epsilon} - \frac{n_{\alpha}(n_{\alpha}+2)(n_{\alpha}-\ell_{\alpha}+1)}{(2n_{\alpha}+1)} \frac{N_{\alpha}}{N_{\alpha+\epsilon}} P_{\alpha+\epsilon} \quad (B.6)$$

We now insert (B.6) into (B.3), multiply through using $Y_{\gamma}^*/4\pi$, and integrate over the unit sphere to get

$$\begin{aligned} \frac{1}{4\pi} \int_0^{2\pi} \int_{-1}^1 (\nabla \cdot \mu \nabla A) Y_{\gamma}^* d\mu d\lambda &= \sum_{\substack{\alpha \\ \ell_{\alpha}=\ell_{\gamma}}} a_{\alpha} \left[\frac{(1-n_{\alpha}^2)(n_{\alpha}+\ell_{\alpha})}{(2n_{\alpha}+1)} \frac{N_{\alpha}}{N_{\alpha-\epsilon}} \right] \frac{1}{2} \int_{-1}^1 P_{\alpha-\epsilon} P_{\gamma} d\mu - \\ &- \sum_{\substack{\alpha \\ \ell_{\alpha}=\ell_{\gamma}}} a_{\alpha} \left[\frac{n_{\alpha}(n_{\alpha}+2)(n_{\alpha}-\ell_{\alpha}+1)}{(2n_{\alpha}+1)} \frac{N_{\alpha}}{N_{\alpha+1}} \right] \frac{1}{2} \int_{-1}^1 P_{\alpha+\epsilon} P_{\gamma} d\mu \end{aligned}$$

$$\begin{aligned}
&= (1-n_Y^2) \left[\frac{(n_Y + \ell_Y)(n_Y - \ell_Y)}{(2n_Y - 1)(2n_Y + 1)} \right]^{1/2} a_{Y-\epsilon} - \\
&- n_Y(n_Y + 2) \left[\frac{(n_Y + \ell_Y + 1)(n_Y - \ell_Y + 1)}{(2n_Y + 1)(2n_Y + 3)} \right] a_{Y+\epsilon} \\
&= D_Y a_{Y-\epsilon} - E_Y a_{Y+\epsilon}
\end{aligned} \tag{B.7}$$

where we have defined

$$\begin{aligned}
D_Y &\equiv (1-n_Y^2) \left[\frac{(n_Y + \ell_Y)(n_Y - \ell_Y)}{(2n_Y - 1)(2n_Y + 1)} \right]^{1/2} \\
E_Y &\equiv n_Y(n_Y + 2) \left[\frac{(n_Y + \ell_Y + 1)(n_Y - \ell_Y + 1)}{(2n_Y + 1)(2n_Y + 3)} \right]^{1/2}
\end{aligned} \tag{B.8}$$

A special case of (B.7) occurs when we consider scalar B in which

$$B = \nabla^2 A \tag{B.9}$$

where similar to (B.2) we can expand B in the form

$$B = \sum_{\alpha} b_{\alpha} Y_{\alpha}(\lambda, \mu). \tag{B.10}$$

Then, from (4.6), we know that

$$b_{\alpha} = -c_{\alpha} a_{\alpha} \tag{B.11}$$

and, in terms of coefficients b_{α} , (B.7) becomes

$$\frac{1}{4\pi} \int_0^{2\pi} \int_{-1}^1 (\nabla \cdot \mu \nabla A) \gamma_Y^* d\mu d\lambda = -\frac{D_Y}{c_{Y-\epsilon}} b_{Y-\epsilon} + \frac{E_Y}{c_{Y+\epsilon}} b_{Y+\epsilon} \quad (\text{B.12})$$

$$= D_Y b_{Y-\epsilon} - E_Y b_{Y+\epsilon}$$

in which we have defined

$$D_Y = -\frac{D_Y}{c_{Y-\epsilon}}, \quad E_Y = -\frac{E_Y}{c_{Y+\epsilon}} \quad (\text{B.13})$$

provided that in (B.12) we ignore terms in which $c_{Y-\epsilon} = 0$ (i.e., $n_{Y-\epsilon} = 0$). Further, for both (B.7) and (B.13) we must stipulate that all terms calling for any $a_{Y-\epsilon}$, $a_{Y+\epsilon}$, $b_{Y-\epsilon}$ or $b_{Y+\epsilon}$ outside the range of the particular spectral truncation chosen must also be ignored.

Reference

Jahnke, E. and F. Emde, 1945: Tables of Functions. Dover, New York, 306 pp. plus tables.

Appendix C. Solution of a tridiagonal set of equations.

Suppose we have an equation set of the form

$$\begin{aligned} a_Y X_{Y-1} + b_Y X_Y + c_Y X_{Y+1} &= R_Y \\ \gamma &= 1, 2, 3, \dots, \Gamma \end{aligned} \tag{C.1}$$

where we must have

$$\left. \begin{aligned} a_1 &= 0 \\ c_\Gamma &= 0 \end{aligned} \right\} \tag{C.2}$$

That is, in matrix form we can write (C.1) as

$$AX = R \tag{C.3}$$

with A being tridiagonal of the form

$$A = \begin{pmatrix} b_1 & c_1 & \dots & \dots & \dots & 0 \\ a_2 & b_2 & c_2 & & & \\ \vdots & \ddots & \ddots & \ddots & & \\ \vdots & & a_\gamma & b_\gamma & c_\gamma & \\ \vdots & & & & & \\ 0 & \dots & \dots & \dots & a_\Gamma & b_\Gamma \end{pmatrix} \tag{C.4}$$

For solutions we define

$$\left. \begin{aligned} C_1 &= 1/b_1 \\ C_\gamma &= 1/(b_\gamma - a_\gamma c_{\gamma-1} C_{\gamma-1}); \quad 2 \leq \gamma \leq \Gamma \\ D_\gamma &= -c_\gamma C_\gamma \end{aligned} \right\} \tag{C.5}$$

and let

$$\left. \begin{aligned} B_1 &= C_1 R_1 \\ B_\gamma &= C_\gamma (R_\gamma - a_\gamma B_{\gamma-1}); 2 \leq \gamma \leq \Gamma \end{aligned} \right\} \quad (C.6)$$

Then, the solutions appear as

$$\left. \begin{aligned} X_\Gamma &= B_\Gamma \\ X_\gamma &= D_\gamma X_{\gamma+1} + B_\gamma; \gamma = \Gamma-1, \Gamma-2, \dots, 1 \end{aligned} \right\} \quad (C.7)$$

provided all C_γ in (C.5) are finite. That is, if

$$\left. \begin{aligned} b_1 &\neq 0 \\ b_\gamma &\neq a_\gamma c_{\gamma-1} c_{\gamma-1} \end{aligned} \right\} \quad (C.8)$$

Appendix D. Computation of the weight functions for Gaussian quadrature.

We consider the set of complete orthogonal Legendre polynomials, $P_n^\ell(\mu)$, in which $\ell = 0, \pm 1, \pm 2, \dots$ and $n = 0, 1, 2, \dots$. We define this set, according to (4.8), to be normalized such that

$$\int_{-1}^1 P_n^\ell(\mu) P_{n'}^{\ell'}(\mu) d\mu = 2\delta_{n,n'} \quad (D.1)$$

where μ is the sine of latitude or equivalently, the cosine of colatitude, ϕ . Now in order to expand an arbitrary function of latitude, say $f(\mu)$, in terms of the set of Legendre polynomials we let

$$f(\mu) = \sum_{\ell n} f_n^\ell P_n^\ell(\mu) \quad (D.2)$$

from which the coefficients, f_n^ℓ , are obtained through application of (D.1) such that

$$f_n^\ell = \frac{1}{2} \sum_{\ell' n'} f_{n'}^{\ell'} \int_{-1}^1 P_{n'}^{\ell'}(\mu) P_n^\ell(\mu) d\mu = \frac{1}{2} \int_{-1}^1 f(\mu) P_n^\ell(\mu) d\mu \quad (D.3)$$

However, to be able to transform at will between spectral and grid point space, it is necessary to represent $f(\mu)$ at a number of discrete points, μ_k , in which $k = 1, 2, 3, \dots, N$ with N being the total number of points lying within $-1 < \mu < 1$. Thus at each latitude point, (D.2) becomes

$$f(\mu_k) = \sum_{\ell n} f_n^\ell P_n^\ell(\mu_k) \quad (D.4)$$

This means that in order to determine coefficients f_n^ℓ we must evaluate the inte-

grals in (D.3) numerically and at the same time maintain the orthogonality properties of the discrete polynomials representation in (D.4). For this purpose, integrating by quadratures, we introduce a set of Gaussian weight functions, w_k , such that

$$\sum_{k=1}^N w_k P_n^\ell(\mu_k) P_{n'}^\ell(\mu_k) \equiv \int_{-1}^1 P_n^\ell(\mu) P_{n'}^\ell(\mu) d\mu \quad (D.5)$$

and the numerical analog for (D.3) becomes

$$\begin{aligned} f_n^\ell &= \frac{1}{2} \sum_{\ell} \sum_n f_n^\ell \sum_{k=1}^N w_k P_n^\ell(\mu_k) P_n^\ell(\mu_k) \\ &= \frac{1}{2} \sum_{k=1}^N w_k f(\mu_k) P_n^\ell(\mu_k) \end{aligned} \quad (D.6)$$

The remainder of this Appendix is devoted to the method of evaluation of the Gaussian weights, w_k .

Because we know that any given Legendre polynomial, $P_n^\ell(\mu)$, can be represented by a finite series in μ of at most degree n , we can expand

$$\begin{aligned} P_n^\ell(\mu) P_{n'}^\ell(\mu) &= \sum_{i=0}^{n+n'} b_i \mu^i \\ \text{or} \quad P_n^\ell(\mu_k) P_{n'}^\ell(\mu_k) &= \sum_{i=0}^{n+n'} b_i [\mu_k]^i \end{aligned} \quad (D.7)$$

and thus,

$$\int_{-1}^1 P_n^\ell(\mu) P_{n'}^\ell(\mu) d\mu = \sum_{i=0}^{n+n'} b_i \int_{-1}^1 \mu^i d\mu \quad (D.8)$$

Integrating (D.8) by quadratures using (D.5),

$$\int_{-1}^1 P_n^\ell(\mu) P_{n'}^\ell(\mu) d\mu = \sum_{k=1}^N w_k P_n^\ell(\mu_k) P_{n'}^\ell(\mu_k) \\ = \sum_{k=1}^N w_k \sum_{i=0}^{n+n'} b_i [\mu_k]^i \quad (D.9)$$

Equating (D.8) and (D.9) we have

$$\sum_{i=0}^{n+n'} b_i \int_{-1}^1 \mu^i d\mu = \sum_{k=1}^N w_k \sum_{i=0}^{n+n'} b_i [\mu_k]^i \quad (D.10)$$

and thus for any i such that $0 \leq i \leq n + n'$ it must hold that

$$\int_{-1}^1 \mu^i d\mu = \sum_{k=1}^N w_k [\mu_k]^i \quad (D.11)$$

We see from (D.11) that if we choose the number of latitude points, N , such that $N-1 = n+n'$ then utilizing all $i = 0, 1, 2, \dots, n+n'$ we can form a set of N equations containing N unknown quantities, w_k , for inversion. However, in terms of colatitude, ϕ , we can show that any $\cos j\phi$ (j is an integer) can be expanded in the form

$$\cos j\phi = \sum_{m=0}^{j/2} a_{2m} \mu^{2m} = a_j \mu^j + \sum_{m=0}^{(j/2)-1} a_{2m} \mu^{2m} \\ \text{and} \\ \cos j\phi_k = a_j [\mu_k]^j + \sum_{m=0}^{(j/2)-1} a_{2m} [\mu_k]^{2m} \quad (D.12)$$

Then, inserting (D.12) into (D.11),

$$\begin{aligned} \frac{1}{a_i} \int_{-1}^1 \cos i \phi d\mu - \frac{1}{a_i} \sum_{m=0}^{(i/2)-1} a_{2m} \int_{-1}^1 \mu^{2m} d\mu &= \\ &= \frac{1}{a_i} \sum_{k=1}^N w_k \cos i \phi_k - \frac{1}{a_i} \sum_{m=0}^{(i/2)-1} a_{2m} \sum_{k=1}^N w_k [\mu_k]^{2m} \end{aligned} \quad (D.13)$$

or

$$\begin{aligned} \sum_{k=1}^N w_k \cos i \phi_k &= \int_{-1}^1 \cos i \phi d\mu \\ &= \int_0^\pi \cos i \phi \sin \phi d\phi \\ &= \begin{cases} 0 & \text{for } i \text{ odd} \\ \frac{-2}{i^2-1} & \text{for } i \text{ even} \\ i = 0, 1, 2, \dots, n+n' \end{cases} \end{aligned} \quad (D.14)$$

where we have made use of (D.11) to eliminate the second term on each side of (D.13). Again, as for (D.11), we see that if we take $N-1 = n+n'$, we can invert (D.14) to obtain the Gaussian weights.

As an example, consider $N=3$ where we select $\phi_1=30^\circ$, $\phi_2=90^\circ$, and $\phi_3=150^\circ$. Then, from (D.14) we can construct the set (using $i = 0, 1, 2$)

$$\left\{ \begin{array}{l} w_1 + w_2 + w_3 = 2 \\ \frac{\sqrt{3}}{2} w_1 - \frac{\sqrt{3}}{2} w_3 = 0 \\ \frac{1}{2} w_1 - w_2 + \frac{1}{2} w_3 = -2/3 \end{array} \right. \quad (D.15)$$

with solutions

$$\left. \begin{aligned} w_1 &= w_3 = 4/9 \\ w_2 &= 10/9 \end{aligned} \right\} \quad (D.16)$$

We note that the solutions (D.16) are symmetric in w_k about the equator. If we assume such symmetry a priori then all equations in (D.14) involving odd values of i become redundant and we can write (D.14) over the integration interval from $\phi = 0$ to $\phi = \pi/2$ as

$$\left. \begin{aligned} \sum_{k=1}^{\frac{N+1}{2}} w_k \cos 2i\phi_k &= \int_0^{\pi/2} \cos 2i\phi \sin \phi d\phi \\ &= -\frac{1}{4i^2-1}; \\ i &= 0, 1, 2, \dots, \frac{n+n'}{2}; N-1 = n+n' \end{aligned} \right\} \quad (D.17)$$

Again, using the example used above in which $N=3$, $\phi_1 = 30^\circ$, and $\phi_2 = 90^\circ$, we have $\frac{N+1}{2} = 2$ and $\frac{N-1}{2} = 1$ giving the set

$$\left\{ \begin{aligned} w_1 + w_2 &= 1 \\ \frac{1}{2}w_1 - w_2 &= -\frac{1}{3} \end{aligned} \right\}$$

with solutions

$$\left. \begin{aligned} w_1 &= \frac{4}{9} \\ w_2 &= \frac{5}{9} \end{aligned} \right\} \quad (D.18)$$

Furthermore, if we want to obtain w_k 's for the entire pole to pole integration, we need only make use of the symmetry property

$$w_{N+1-k} = w_k + \delta_{\phi_k, \pi/2} w_k \quad (\text{D.19})$$

which gives for our example

$$\left. \begin{aligned} w_1 &= w_3 = \frac{4}{9} \\ w_2 &= \frac{5}{9} + \frac{5}{9} = \frac{10}{9} \end{aligned} \right\} \quad (\text{D.20})$$

Solutions (D.20) are identical with those of (D.16).